PART III GEOCHEMICAL PROSPECTING

PART III GEOCHEMICAL PROSPECTING

Chapter 1 Sampling and Analytical Method

1-1 Sampling

Sampling was conducted throughout the area with the exception of the carbonates in the northern part where detailed geochemical data have been obtained by MINDECO/NORANDA and the northwestern margin where thick alluvium covers the geologic units.

Many of the ore deposits and mineralization occur in carbonate rocks. Therefore, we conducted dense sampling in the carbonates of the eastern part with 1 km interval in N-S and 500m interval in E-W direction. In other parts of the area sampling interval was 2 km in N-S and 500 m in E-W direction. Five hundred samples were collected altogether.

First we selected the intersection of the Kaindu Road and the Lubungu Pontoon Road as the base point and set sampling points every 500 m along the road using odometer and sampled the points which were not artificially poluted. The sample numbers were marked on nearby large trees and these served as reference points. Other sampling points were determined by selecting routes close to the UTM grid of the 1:50,000 topographic map using the above reference points, measuring rope and clinocompas (Fig. III-1).

The method of sampling is as follows; we dug a hole 30cm-50cm deep, eliminated A and B horizons of the humic soil and sampled the C horizon. The samples were dried in air at the spot, collected two batches, 50g each, of -80 mesh size, combined them, halved it by quartering and sent

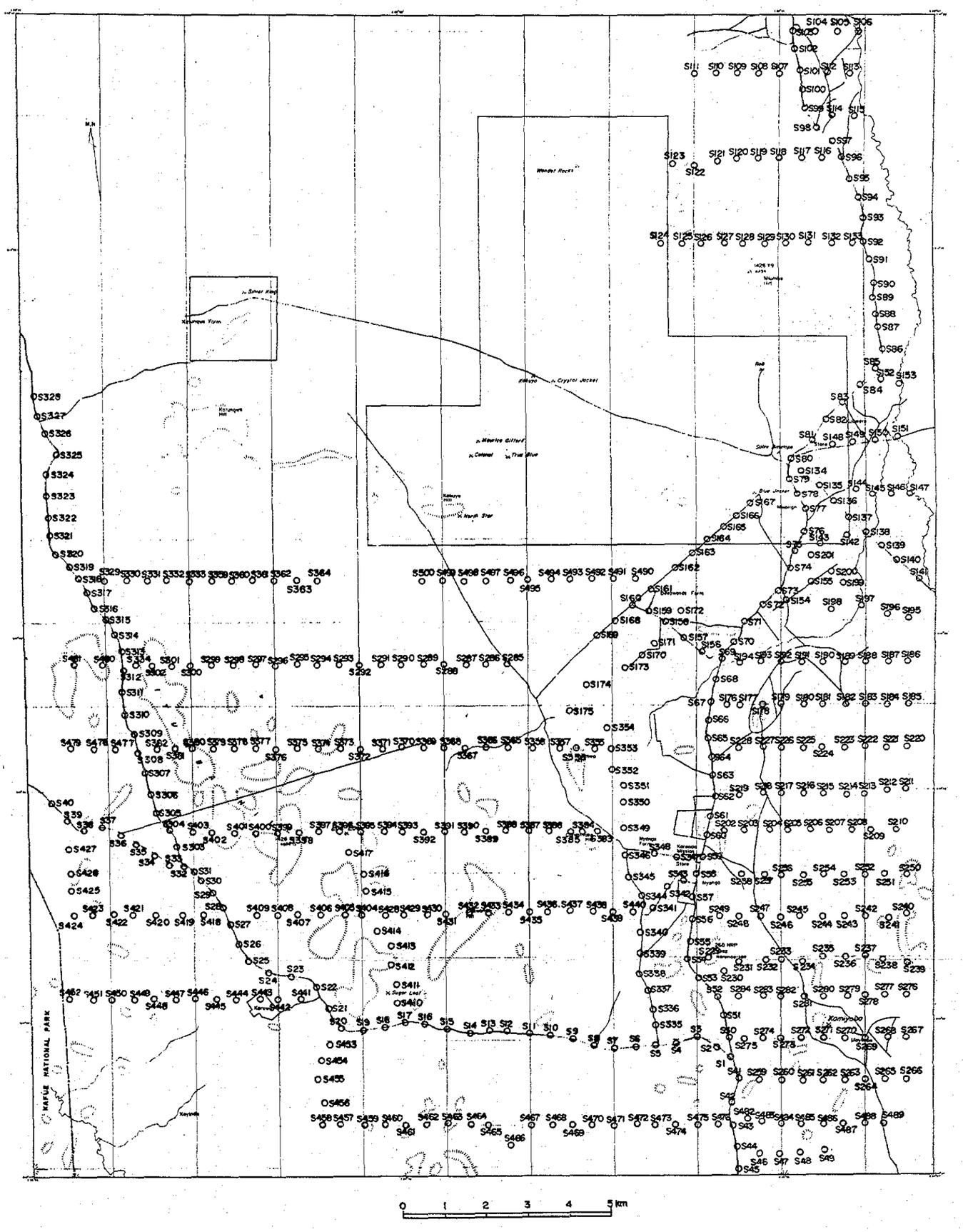

Fig. Ⅲ－1 Location Map of Geochemical Samples (Soil)

one for analysis and the other was kept at MINEX for reference.

1-2 Analytical Method

1-2-1 Indicator Elements

Silver, copper and zinc mineralizations are known in the surveyed area. The indicators used by MINDECO/NORANDA many years back, namely Cu-Zn showed significant geochemical anomalies and reflected the old mines and known mineralized zones very well. Thus in the present survey, we used Cu, Pb, Zn and Ag as the indicator elements.

1-2-2 Analytical Methods

We used atomic absorption method for analysis, used mixture of HNO_3 and $HClO_4$ as stabilizer for Cu, Pb, Zn and HNO_3 for Ag. The procedure is laid out in Fig. III-2.

Chapter 2 Data Processing and Interpretation

2-1 Data Processing

The analytical results were studied and processed by the procedure advocated by C. Lepeltier (1969) (Fig. III-3). Then anomalies and anomalous zones were extracted.

2-2 Quality of Data

Of the analytical data of 500 samples (Ap.6), only 13

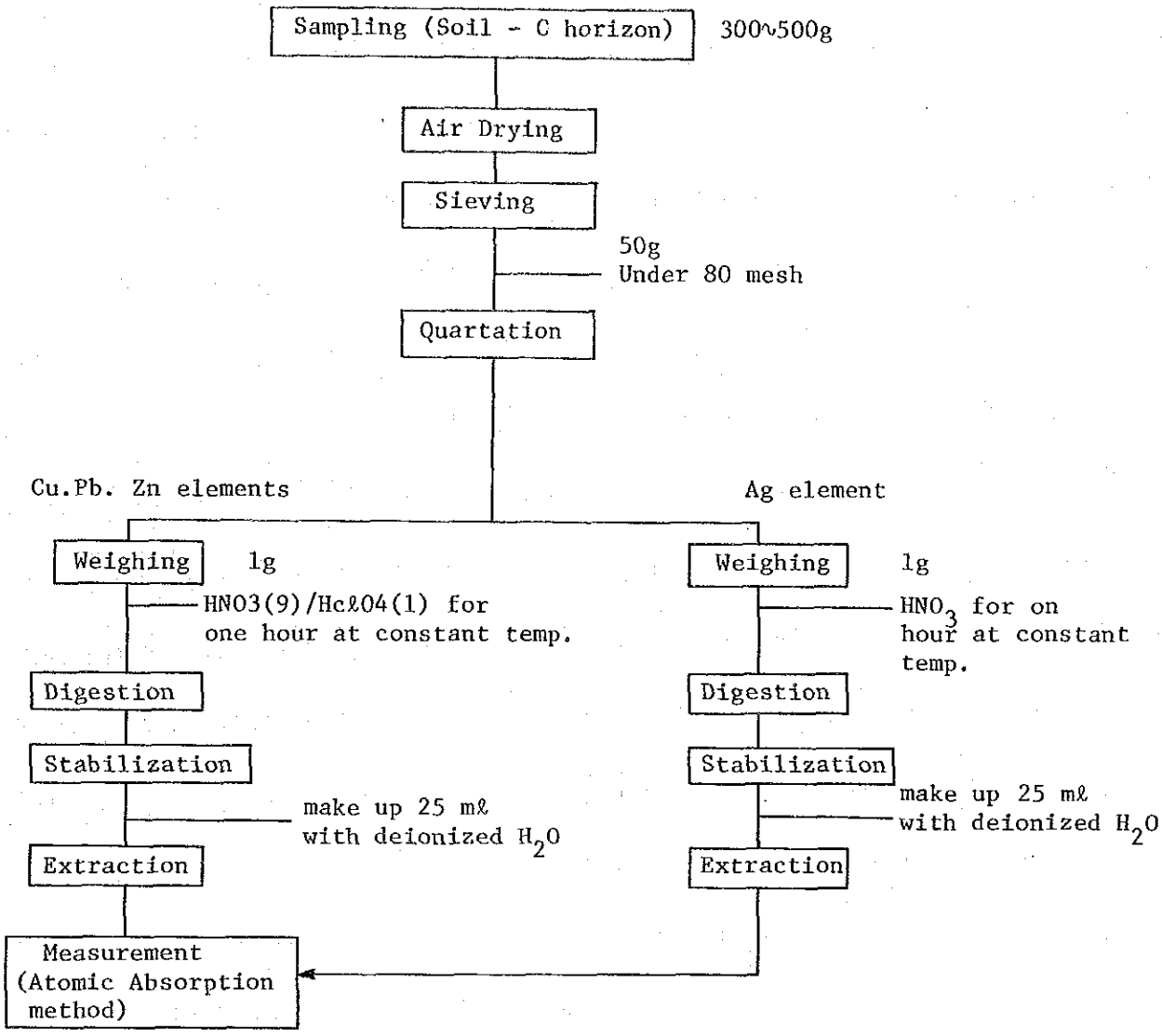

(Detection limit)

Cu,Pb, Zn	Ag
1 ppm	1g/t

Fig. Ⅲ -2 Flow Chart for Pretreatment and Chemical Analysis of Geochemical Samples

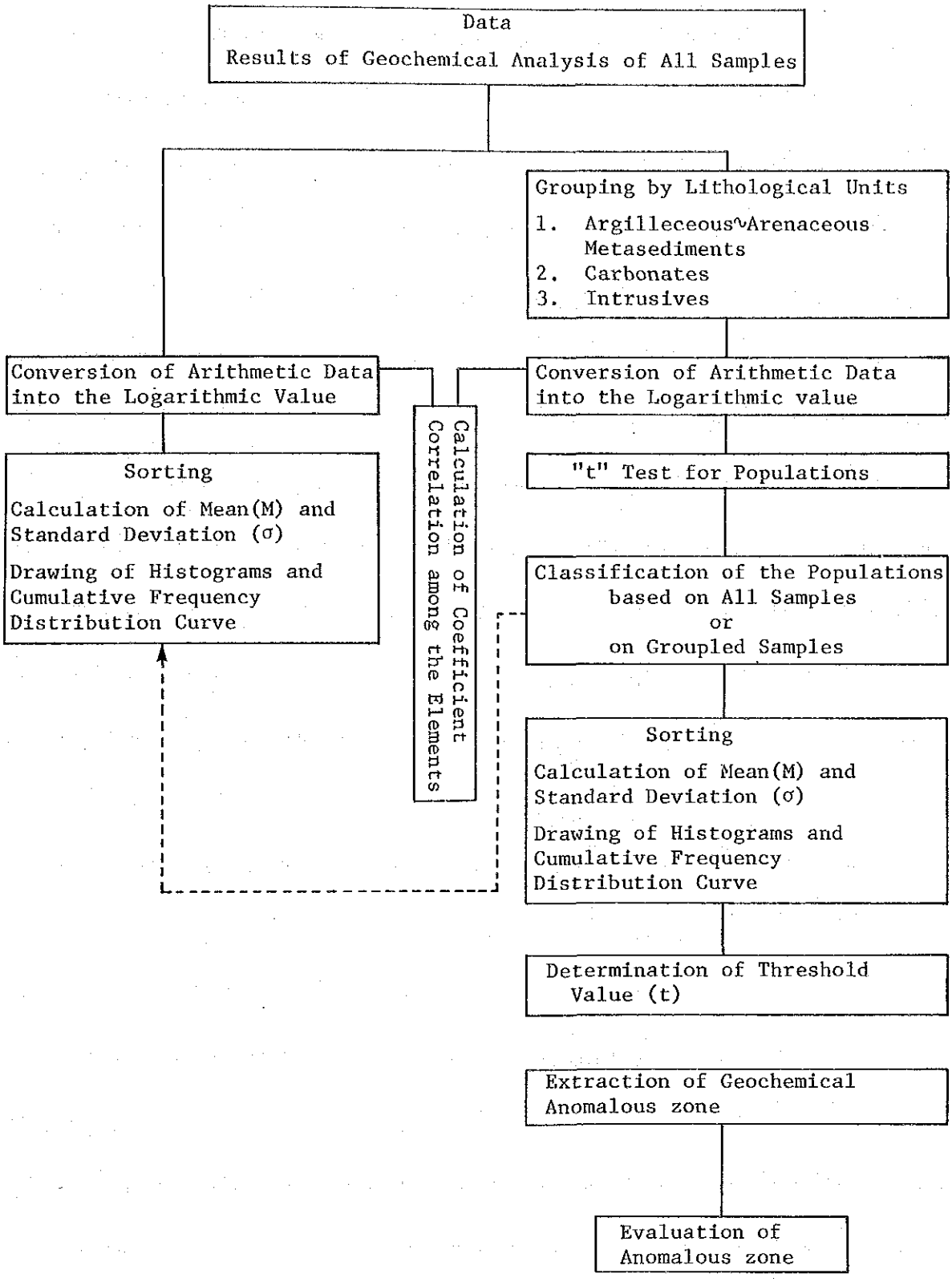

Fig. Ⅲ-3 Flow Chart of Statistical Treatment of Geochemical Data

showed Ag values higher than 1 ppm, this is 2.6% of the total.

Generally, the content of Ag is 0.1 ppm in soils and 0.3 ~ 0.5 ppm in igneous rocks. The background value of the surveyed area is considered to be higher than the general values because it is close to ore deposits and igneous rocks are developed. Therefore, we considered the samples with over 1 ppm Ag as anomalies and excluded them from statistical process which was carried out for Cu, Pb and Zn.

The geology of this area can be divided lithologically into the following three groups.

1. Argillaceous-arenaceous metasediments, 2. carbonates, 3. intrusive rocks (syenites and quartz porphyry). The number of samples collected from these lithologic groups are as follows.

1.	Argillaceous-arenaceous metasediments	327 samples
2.	Carbonates	74 samples
3.	Intrusives	99 samples
	Total	500 samples

First, we investigated whether there were any significant difference in the mean values of the above three populations by the following calculation.

1. Hypothesis;

   $Ho: \mu_x = \mu_y$ (Mean values of the two populations are equal)

2. Calculate $\hat{\sigma}$ after suming the square values S_x, S_y, by ;

$$\hat{\sigma} = \sqrt{\frac{S_x + S_y}{n_x + n_y - 2}}$$

3. Obtain t_0 by;

$$t_0 = \frac{\bar{x} - \bar{y}}{\sqrt{\frac{1}{n_x} + \frac{1}{n_y}} \cdot \hat{\sigma}}$$

4. Result;

There are differences between the mean values of the populations μ_x and μ_y if $|t_0| \geq t(n_x + n_y - 2,005)$

The results are as follows.

The difference of mean values of population by lithology

	Argillaceous ~Arenaceous metasediments : Carbonates	Argillaceous ~Arenaceous metasediments : Intrusives	Carbonates : Intrusives
Cu	×	○	○
Pb	○	○	×
Zn	○	×	○

○ Significant difference exists with 95% reliability

X Significant difference does not exist with 95% reliability

Although there are no difference of the mean values of Cu in argillaceous-arenaceous metasediments and carbonates, Zn in the metasediments and intrusives, and Pb in carbonates and intrusives; significant differences exist among other combinations.

It was proven above that the collected samples showed different mean values for the three lithologically classified groups. Therefore the data were processed separately for each lithologic groups. Also the correlation of the elements are as follows.

Rock Unit	Amount of Samples	Elements	Coefficient of correlations
Argillaceous ~Arenaceous metasediments	327	Cu – Zn	•695940
		Cu – Pb	•766132
		Pb – Zn	•861135
Carbonates	74	Cu – Zn	•338802
		Cu – Pb	•573899
		Pb – Zn	•624339
Intrusives	99	Cu – Zn	•445525
		Cu – Pb	•563532
		Pb – Zn	•756473

Very good correlation is observed between all elements, particularly high correlation exists for Pb-Zn followed by Cu-Pb and Cu-Zn.

The correlation for all samples are as follows.

Rock unit	Amount of samples	Elements	Coeffcient of correlations
All units	500	Cu – Zn	•581253
		Cu – Pb	•713854
		Pb – Zn	•802099

The result is the same as in the case for the three independent population.

2-3 Statistical Treatment of Data

All analytical data were converted to logarithmic values and histograms and cumulative frequency distribution curves were prepared (Figs. Ⅲ-4 ~ 7).

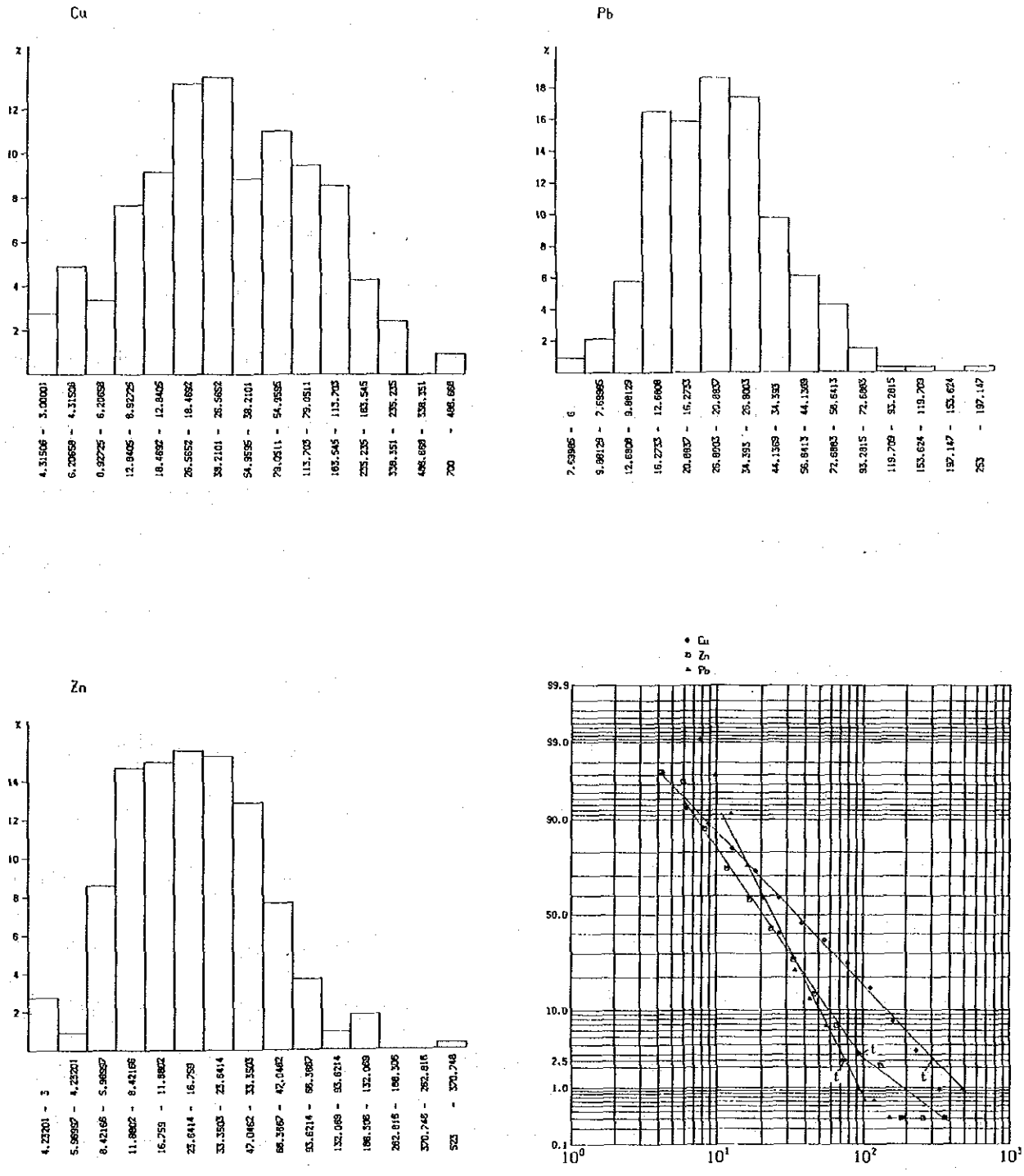

Fig. III-4 Histogram and Cumulative Frequency Distribution Curve of Geochemical Data of Argillaceous ∿ Arenaceous Metasediments

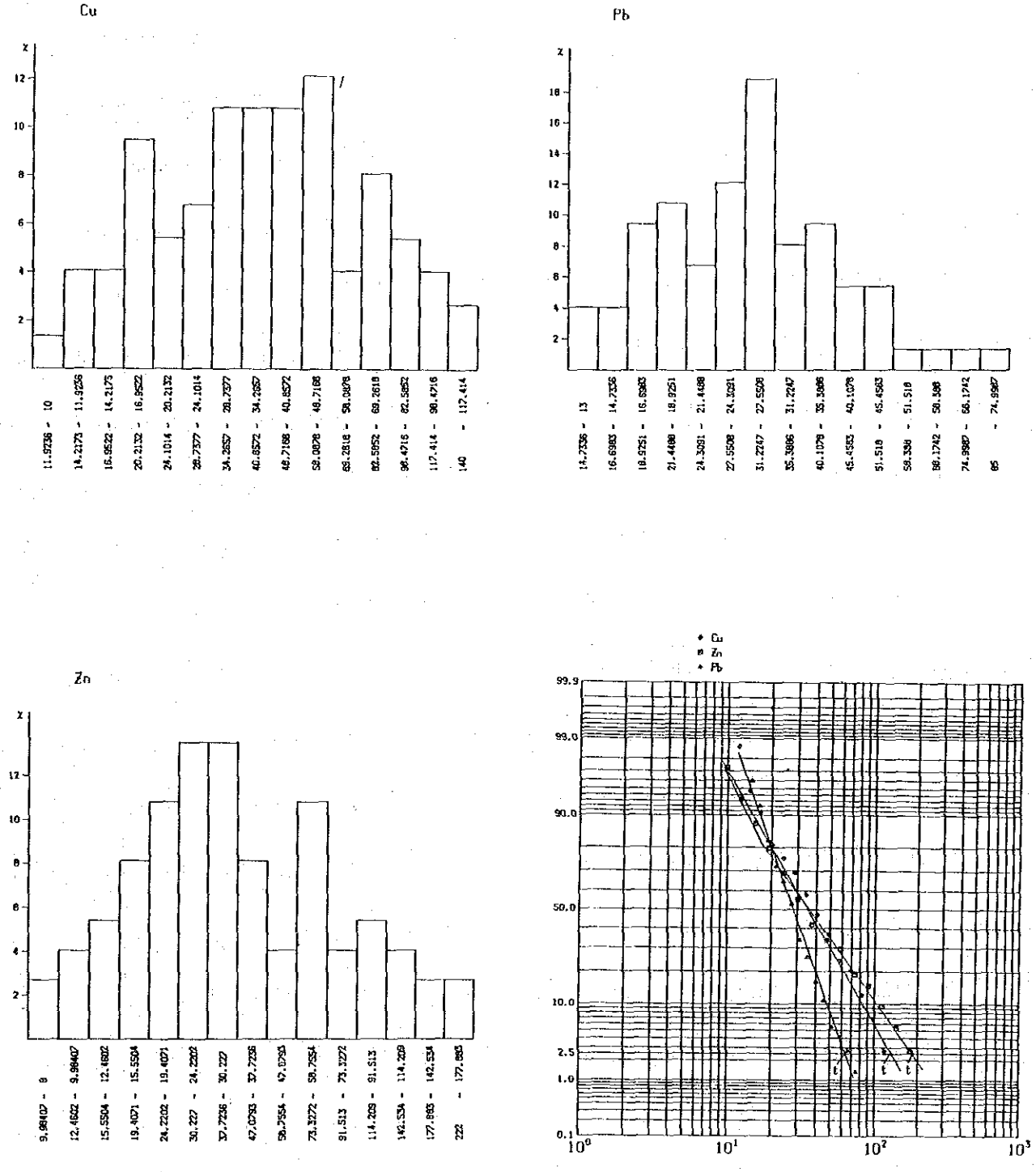

Fig.Ⅲ-5 Histogram and Cumulative Frequency Distribution Curve of Geochemical Data of Carbonates

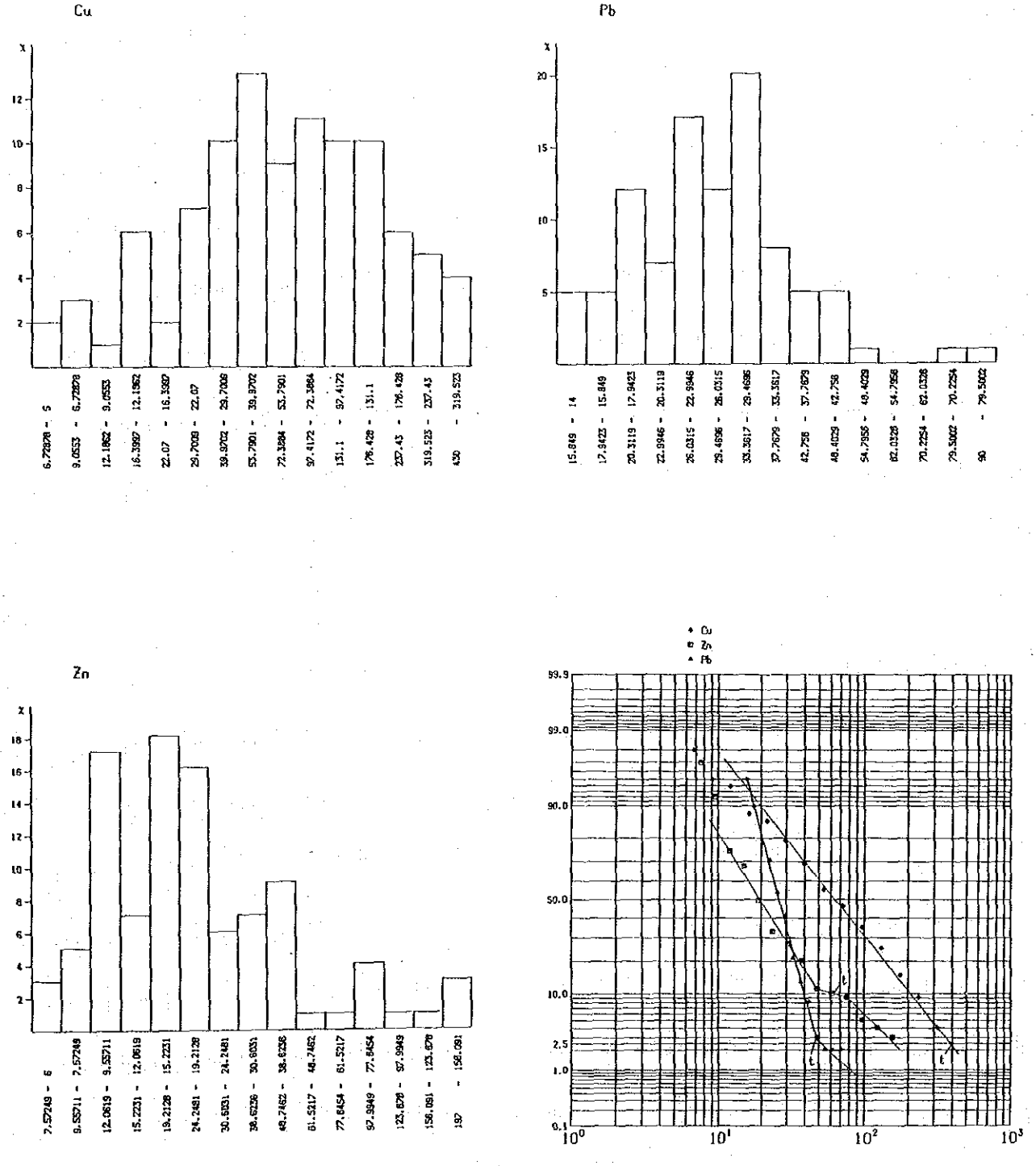

Fig. Ⅲ-6 Histogram and Cumulative Frequency Distribution Curve of Geochemical Data of Intrusives

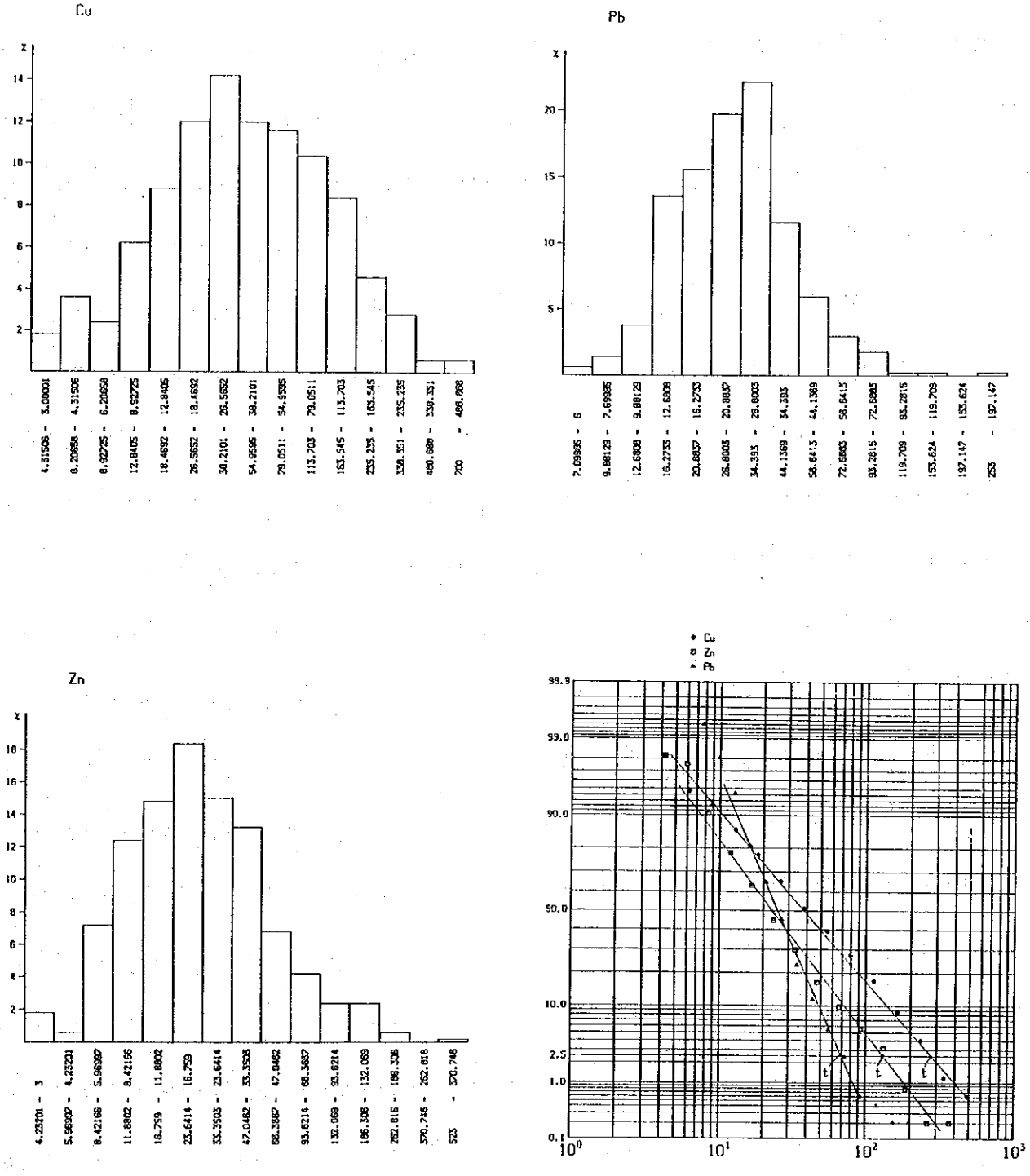

Fig.Ⅲ—7 Histogram and Cumulative Frequency Distribution Curve of Geochemical Data of All Rocks

The plots of all elements are close to lognormal distribution. The mean values (M) and the standard deviation (σ) calculated from these distribution are as follows (The values for all samples are listed for reference).

Rock unit	Amount of samples	Element	Mean(M)	Standard deviation(σ)
Argillaceous ~Arenaceous metasediments	327	Cu	34	•479417
		Pb	24	•231199
		Zn	20	•349456
Carbonates	74	Cu	38	•266944
		Pb	27	•167414
		Zn	37	•333302
Intrusives	99	Cu	62	•433765
		Pb	27	•146957
		Zn	21	•325906
All units	500	Cu	39	•455848
		Pb	25	•210091
		Zn	22	•354404

From these figures, order of intrusives>metasediments> carbonates is seen for Cu, all three populations show the same value for Pb and carbonates > intrusives > metasediments for Zn. This fact supports the difference of mean values among different lithologic units.

2-4 Determination of Anomalies

M+σ, M+2σ and the threshold values calculated from mean (M), standard deviation (σ) and cumulative distribution curves for each lithologic unit are as follows.

Rock unit	Element	M + σ	M + 2σ	Threshold Value(t)
Argillaceous ~ Arenaceous metasediments	Cu	105	317	305
	Pb	40	69	73
	Zn	45	102	90
Carbonates	Cu	71	132	137
	Pb	40	60	62
	Zn	80	173	185
Intrusives	Cu	169	460	395
	Pb	38	53	49
	Zn	46	98	62
All units	Cu	113	324	300
	Pb	40	66	70
	Zn	51	115	137

The threshold values were determined from the cumulative frequency distribution curve by adopting the 2.5% point when the line was straight, the bending point when it bend between 2.5 and 10%, and the median of bends when there were two bending points.

The values for all lithologic units are also listed and it is seen that in spite of the extreme values of Cu in intrusive rocks and Zn in carbonates, they are averaged for the whole area.

Before determining the anomalies, we assumed that M+σ, M+2σ and the threshold values as anomalies and considered the anomalous zones for the three lithologic units and also for the case of the whole area as a single population. The result is as follows.

	Population	Anomaly	Nature of Anomalous Zone
①	1 (All samples)	M+σ and M+2σ	The M+σ zone is large while M+2σ zone is very limited and thus clear anomalous zone cannot be delineated. The Cu anomalous zone is concentrated in intrusive rock distribution.
②	" (All samples)	Threshold values (t)	Anomalous zones are extracted but Cu anomalies are concentrated in intrusive rocks as in ①
③	3 (Each lithological unit)	M+σ and M+2σ	Approximately the same as ①
④	" (Each lithological unit)	Threshold values (t)	Anomalous zones are clearly delineated

Thus, it is seen that the only clear method for delineating anomalous zones is by using threashold values (t) of the three separate populations as the anomaly. Therefore, the threshold values of each lithologic units were used as the minimum anomalies.

The values are as follows.

	Cu ppm	Pb ppm	Zn ppm	Ag ppm
Argillaceous~Arenaceous metasediments	≧ 305	≧ 73	≧ 90	≧ 1
Carbonates	≧ 137	≧ 62	≧ 185	≧ 1
Intrusives	≧ 395	≧ 49	≧ 62	≧ 1

Chapter 3 Extraction and Evaluation of Anomalous Zones

3-1 Extraction of Anomalous Zones

The anomalous zones extracted by the equal anomaly lines and the evaluation of these zones are shown in Fig. III-8 and Table III-1.

The anomalous zones in this case are defined as zones with anomalies of two or more elements or those which contain more than two anomalies.

3-2 The Characteristics of the Anomalies and Anomalous Zones

The anomalies and anomalous zones extracted above show some localization for each element. Namely, the Cu anomalies are found in the western part where intrusives, particularly quartz porphyry is predominant; Pb and Zn anomalies in the intrusives of the central part also in the direction of carbonate distribution, N-S, in the eastern part. Ag anomalies are found over lapping the zones of the other elements and very few independent zones are also found.

3-3 Evaluation of Anomalous zones

1. Geochemical Anomalous Zone Near Sable Antelope Disused Mine

This zone belongs to the eastern margin of the anomalous zone including Sable Antelope and Blue Jacket Mineralized Zone extracted by MINDECO/NORANDA some years ago. In the present survey, very few samples were collected for check purposes only, but anomalies such as Zn 222 ppm and Ag 1 ppm were obtained and it was confirmed that it was possible to delineate

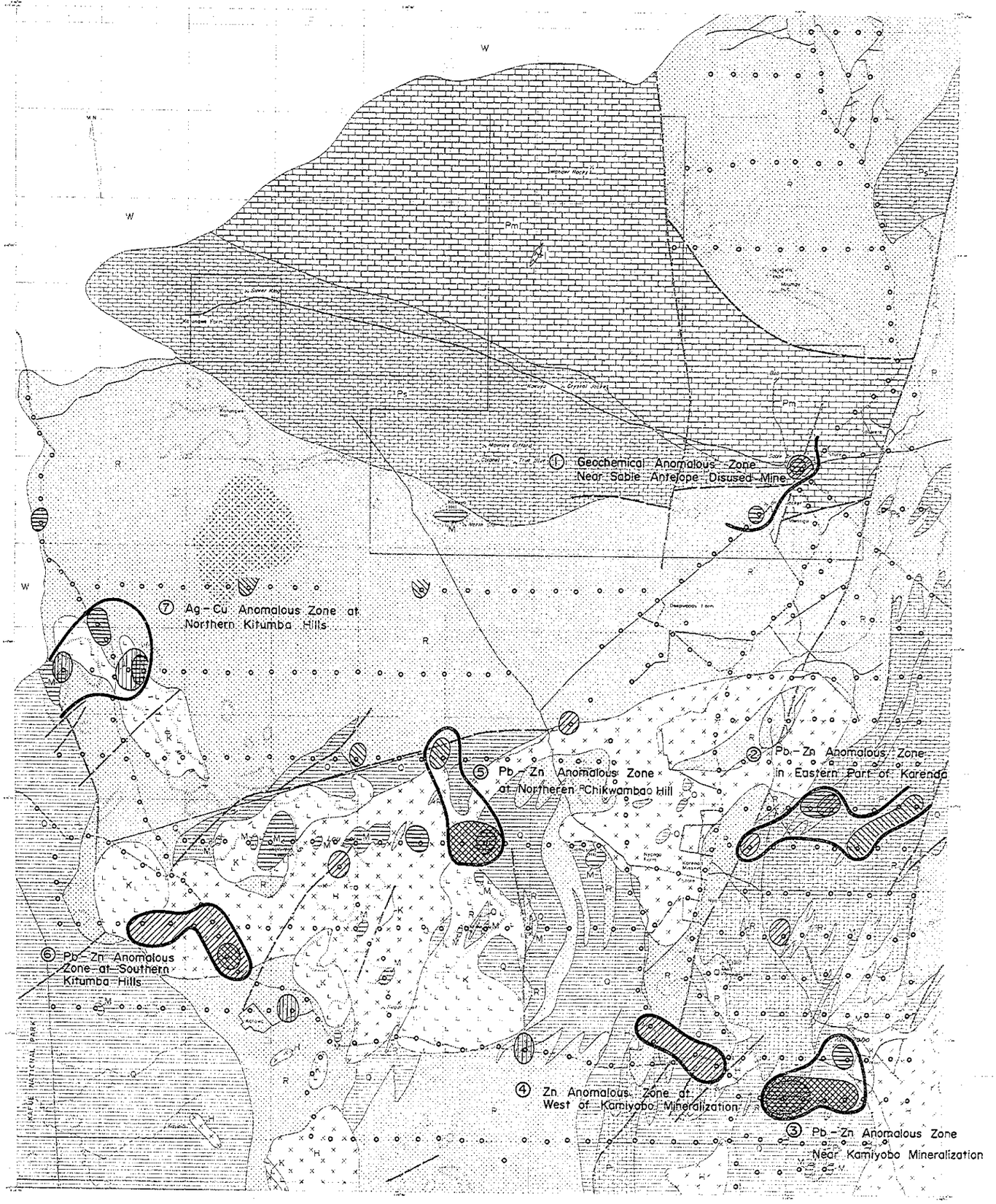

LEGEND

Geochemical Anomalous Zone

Cu
1 : Argillaceous ~ Arenaceous metasediments ≧ 305 ppm
2 : Carbonates ≧ 137 ppm
3 : Intrusives ≧ 395 ppm

Pb
1 : ≧ 73 ppm
2 : ≧ 62 ppm
3 : ≧ 49 ppm

Zn
1 : ≧ 90 ppm
2 : ≧ 185 ppm
3 : ≧ 62 ppm

Ag
≧ 1 ppm

(See Fig. Ⅱ – 1 on Geological Legend)

Fig. Ⅲ – 8 Map of Geochemical Anomalous Zones in the Surveyed Area

Table III -1 The List of Geochemical Anomalous Zones

No.	Anomalous Zone	Amounts of over Critical value(t)		Maximum value (ppm)	Extention of anomalous zone(km)		Rock unit	* Evaluation
		element	≧t		High anomalous zone	Whole zone		
1	Geochemical Anomalous Zone Near Sable Antelope Disused Mine	Cu	-	(230)	-	1.0×0.5	Pm, Ps	-
		Pb	-	(59)	-			
		Zn	1	222	0.5×0.5			
		Ag	2	1	0.5×1.0			
2	Pb-Zn Anomalous Zone in Eastern Part of Karenda	Cu	-	(100)	-	2.0×4.0	Ps	B
		Pb	2	85	2.0×0.5			
		Zn	2	212	0.5×0.5			
		Ag	2	1	0.5×0.5			
3	Pb-Zn Anomalous Zone Near Kamiyobo Mineralization	Cu	-	(290)	-	1.5×2.0	Q, Ps	A
		Pb	3	253	1.0×2.0			
		Zn	3	523	1.0×2.0			
		Ag	3	1	0.5×0.5			
4	Zn Anomalous Zone at West of Kamiyobo Mineralization	Cu	-	(110)	-	0.5×2.0	Q, R	A
		Pb	-	(56)	-			
		Zn	3	147	0.5×2.0			
		Ag	-	1	-			
5	Pb-Zn Anomalous Zone at Northern Chikwamba Hill	Cu	-	(173)	-	3.5×1.0	Q,R, H	B
		Pb	3	90	1.0×1.0			
		Zn	2	197	1.0×1.0			
		Ag	1	1	0.5×0.5			
6	Pb-Zn Anomalous Zone at Southern Kitumba Hill	Cu	-	(260)	-	1.5×2.0	H, K	B
		Pb	1	77	0.5×0.5			
		Zn	6	181	1.5×2.0			
		Ag	-	1	-			
7	Ag-Cu Anomalous Zone at Northern Kitumba Hill	Cu	3	670	0.5×0.5	2.0×2.0	K, R	B
		Pb	-	69	-			
		Zn	-	140	-			
		Ag	3	2	0.5×0.5			

( ): less than critical value

* A: detailed geochemical survey necessary
B: to be studied after the results of A

anomalous zones even by the present sampling interval.

2. Pb-Zn Anomalous Zone in Eastern Part of Karenda

This zone comprises two Pb, Zn and two Ag anomalies. The Pb and Zn anomalies are at separate points and do not overlap. The maximum anomalies are Pb 85 ppm, Zn 212 ppm and Ag 1 ppm.

This zone lies to the north of and is parallel to the anomalous zone near Kamiyobo mineralization (3), but is weaker. Therefore, we concluded that future prospecting in the southeastern part of the surveyed area should be planned after considering the results of the work near Kamiyobo and we evaluated this zone as Rank B.

3. Pb-Zn Anomalous Zone Near Kamiyobo Mineralization

This zone comprises three Pb-Zn anomaly points and also three Ag anomalies. All Pb and Zn anomalies overlap in this zone. The highest anomalies are Pb 253 ppm, Zn 523 ppm and Ag 1 ppm. These values are higher than those of other zones.

The interesting characteristics of this zone is that Pb-Zn anomalies are concentrated at a distance southward from the old Cu workings and the point which is interpreted as the strongest mineralization has not been explored. Also the Cu value is not high enough for anomalies, but the maximum value is 290 ppm and indicates mineralization.

This zone is at the contact of the intrusives and carbonates, it includes old workings of the Kamiyobo mine and the mineral showings of this mine is strong at the surface and there are possibilities of occurrence of new deposits. Therefore, this zone was evaluated

as Rank A.

4. Zn Anomalous Zone at West of Kamiyobo Mineralizatior

Only Zn anomalies occur in this zone. There are three Zn anomalies and the maximum value is 147 ppm. Although only Zn anomalies occur in this zone, this is located at the western extension of the Kamiyobo mineralization whose continuation is anticipated. Therefore, this zone was evaluated as Rank A.

5. Pb-Zn Anomalous Zone at Northern Chikwamba Hill

This zone comprises three Pb anomalies, two Zn anomalies and one Ag anomaly. The Zn and Ag overlap with the Pb anomalies. The maximum values are Pb 90 ppm, Zn 197 ppm and Ag 1 ppm.

The anomalies of this zone are relatively weak, the two traverses on which the anomalies occur are 2 km apart and the continuity of the mineralization is not clear. Therefore this zone was evaluated as Rank B.

6. Pb-Zn Anomalous Zone at Southern Kitumba Hills

This zone comprises six Zn anomalies and one overlapping Pb anomaly. The maximum values are Zn 181 ppm and Pb 77 ppm.

This zone is located where intrusives such as syenites and quartz porphyry are predominant. The number of anomaly readings are large, but the values are not very high and there are no known mineralization nearby. Therefore this zone was evaluated as Rank B.

7. Ag-Cu Anomalous Zone at Northern Kitumba Hills

This zone comprises three Cu and three Ag anomalies. The maximum values are Cu 670 ppm and Ag 2 ppm.

This zone has geologic environment similar to that of the southern Kitumba zone. Although the Cu anomaly values are relatively high, there are no continuity among the anomalies and there are no mineralization nearby. Therefore, this zone was evaluated as Rabk B.

8. Other Anomalies

There are some mono-element anomalies. Copper anomalies occur to the east of Karawa Village and at a mid-point of Lubungu Pontoon Road southeast of chikwamba Hill, Pb anomalies are found at three separate points in the central part of the surveyed area, and Zn anomalies to the south of Lou Lou old workings, at north Karawa Hill and at east Karenda Hill. These one element, one anomaly type of occurrences are of very limited scope and scale and also the values are low. Therefore, these are not considered as anomalous zones.

Chapter 4 Re-analysis of Existing Geochemical Data

As mentioned in Chapter 1, geochemical prospecting was conducted by MINDECO/NORANDA for the carbonate rock area in the northern part of the surveyed area. The traverse interval was 400 m and the sampling interval was 100 m. This area was excluded from sampling during the present work. MINDECO/NORANDA further conducted detailed geochemical

work (100 m traverse interval, 50 m sampling interval) for the anomalous zones extracted from the above survey. These data were processed by the method reported in Chapter 3 and the results are shown in Table Ⅲ-2, Figs.Ⅲ-9, 10. It is seen that for Cu, threshold value (t) is 250 ppm, M+σ 109 ppm, M+2σ 266 ppm, M+3σ 650 ppm, and for Zn, (t) 129 ppm, M+σ 140 ppm, M+2σ 366 ppm, M+3σ 953 ppm. Geochemical anomalous zones extracted from the above values are shown in Fig. Ⅲ-11. Also similar map for Bob Zinc mineralized zone based on Zn values is laid out in Fig. Ⅱ-4.

From these two maps, it is seen that the agreement between geochemical anomalous zones and the ore deposits, mineralization, mineral showings are very good. Also they show the direction of the continuity of mineralization. The Cu anomalous zone extends in N70°~80°W direction from Sable Antelope and Crystal Jacket through Maurice Gifford, Colonel, and North Star to Silver King. These mineralizations are continuous and is generally distributed harmoniously with the geologic structure.

The Zn anomalous zones show good continuity in E-W direction from Blue Jacket to North Star. These anomalies are distributed in harmony with the boundary of carbonates and argillaceous metasediments. There are also independent anomalies of Wonder Rocks and Bob Zinc, they occur at the intersections of E-W and N-S trending anomalous zones. The Wonder Rocks mineralization trends mainly in N80°E direction with minor elongation in N20°W direction. At the Bob Zinc mineralization N70°W is the major elongation with the addition of N-S direction continuing from Sable Antelope.

Table Ⅲ-2 Statistical Data of Geochemical Samples in Northern Part of the Surveyed Area

		Class	Frequency	Cumulative frequency
Cu	1	14000.00000 - 8247.40000	1(0.02%)	1(0.02%)
	2	8247.40000 - 4858.55000	1(0.02%)	2(0.05%)
	3	4858.55000 - 2862.17000	0(0.00%)	2(0.05%)
	4	2862.17000 - 1686.11000	0(0.00%)	2(0.05%)
	5	1686.11000 - 993.28900	8(0.19%)	10(0.24%)
	6	993.28900 - 585.14700	22(0.54%)	32(0.78%)
	7	585.14700 - 344.71000	34(0.83%)	66(1.61%)
	8	344.71000 - 203.06900	135(3.28%)	201(4.89%)
	9	203.06900 - 119.62800	397(9.66%)	598(14.55%)
	10	119.62800 - 70.47300	551(13.41%)	1149(27.96%)
	11	70.47300 - 41.51570	868(21.12%)	2017(49.08%)
	12	41.51570 - 24.45690	1201(29.22%)	3218(78.30%)
	13	24.45690 - 14.40760	650(15.82%)	3868(94.11%)
	14	14.40760 - 8.48752	175(4.26%)	4043(98.37%)
	15	8.48752 - 5.00001	67(1.63%)	4110(100.00%)
Zn	1	12000.00000 - 7142.23000	2(0.05%)	2(0.05%)
	2	7142.23000 - 4250.95000	0(0.00%)	2(0.05%)
	3	4250.95000 - 2530.10000	2(0.05%)	4(0.10%)
	4	2530.10000 - 1505.88000	2(0.05%)	6(0.15%)
	5	1505.88000 - 896.28000	24(0.58%)	30(0.73%)
	6	896.28000 - 533.45300	57(1.39%)	87(2.12%)
	7	533.45300 - 317.50400	112(2.73%)	199(4.84%)
	8	317.50400 - 188.97400	174(4.23%)	373(9.08%)
	9	188.97400 - 112.47400	392(9.54%)	765(18.61%)
	10	112.47400 - 66.94310	799(19.44%)	1564(38.05%)
	11	66.94310 - 39.84360	1161(28.25%)	2725(66.30%)
	12	39.84360 - 23.71440	633(15.40%)	3358(81.70%)
	13	23.71440 - 14.11450	528(12.85%)	3886(94.55%)
	14	14.11450 - 8.40072	195(4.74%)	4081(99.29%)
	15	8.40072 - 4.99999	29(0.71%)	4110(100.00%)

Element	Population	Maximum value	Minimum value	Mean(M)	Standard deviation (σ)	M+σ	M+2σ	M+3σ	Threshold value (t)
Cu	4110	ppm 14000	ppm 5	44	.38771	109	266	650	250
Zn	4110	ppm 12000	ppm 5	54	.415258	140	366	953	129

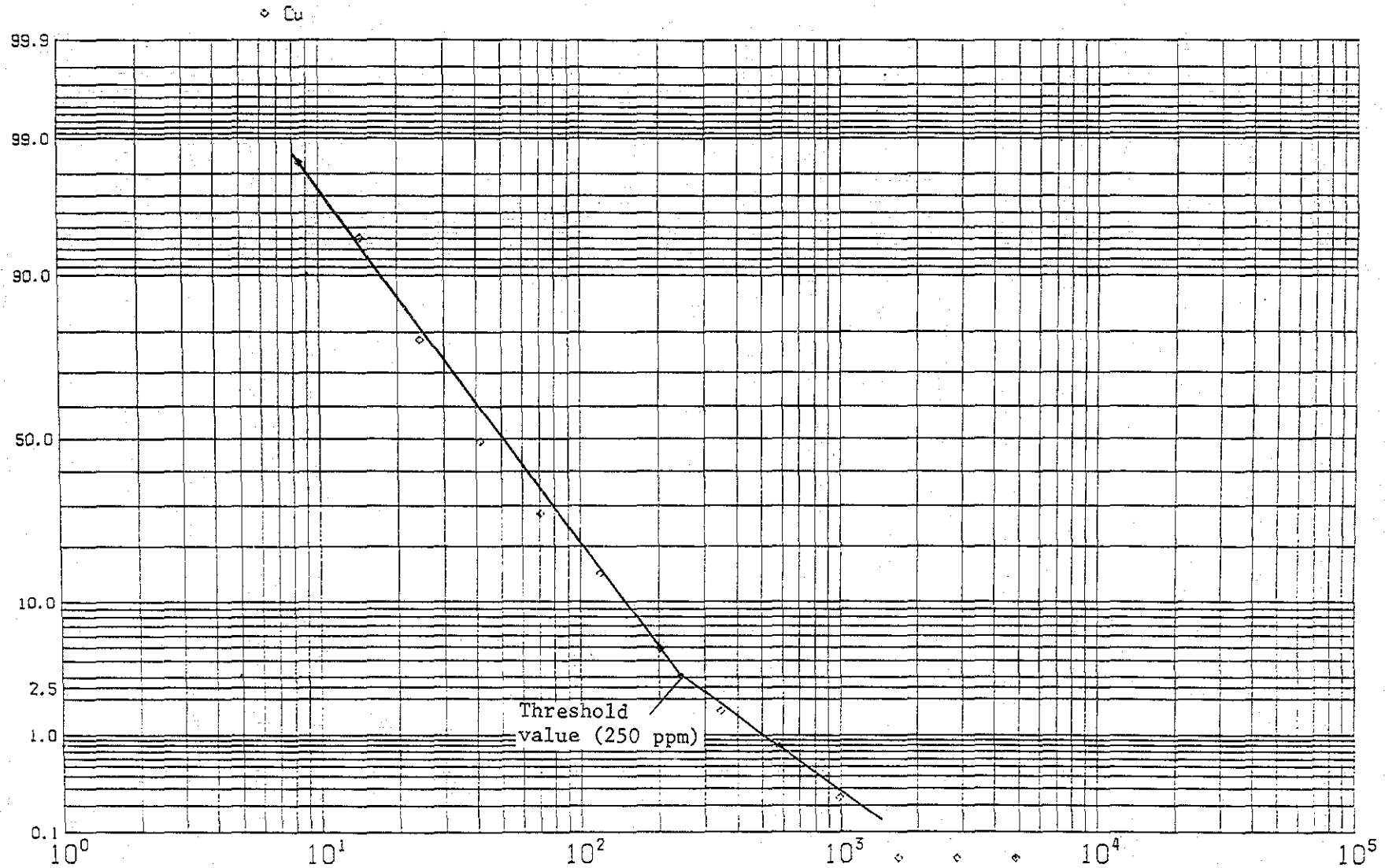

Fig.III-9 Cumulative Frequency Distribution Curve of Geochemical Data in Northern Part of the Surveyed Area (Cu)
(Sampled and assayed by Mindeco Noranda Ltd.)

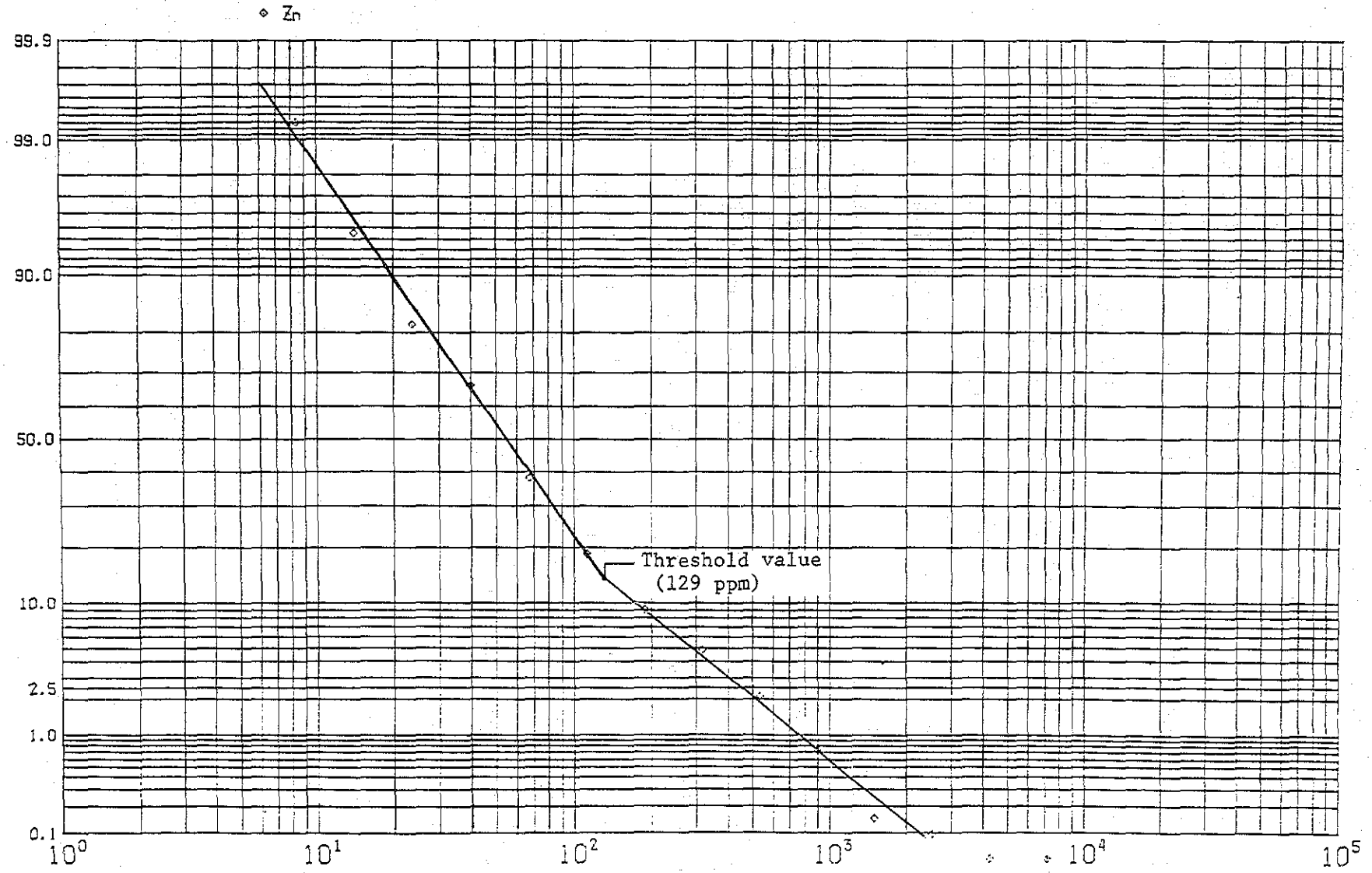

Fig.III－10 Cumulative Frequency Distribution Curve of Geochemical Data in Northern Part of the Surveyed Area (Zn)
(Sampled and assayed by Mindeco Noranda Ltd.)

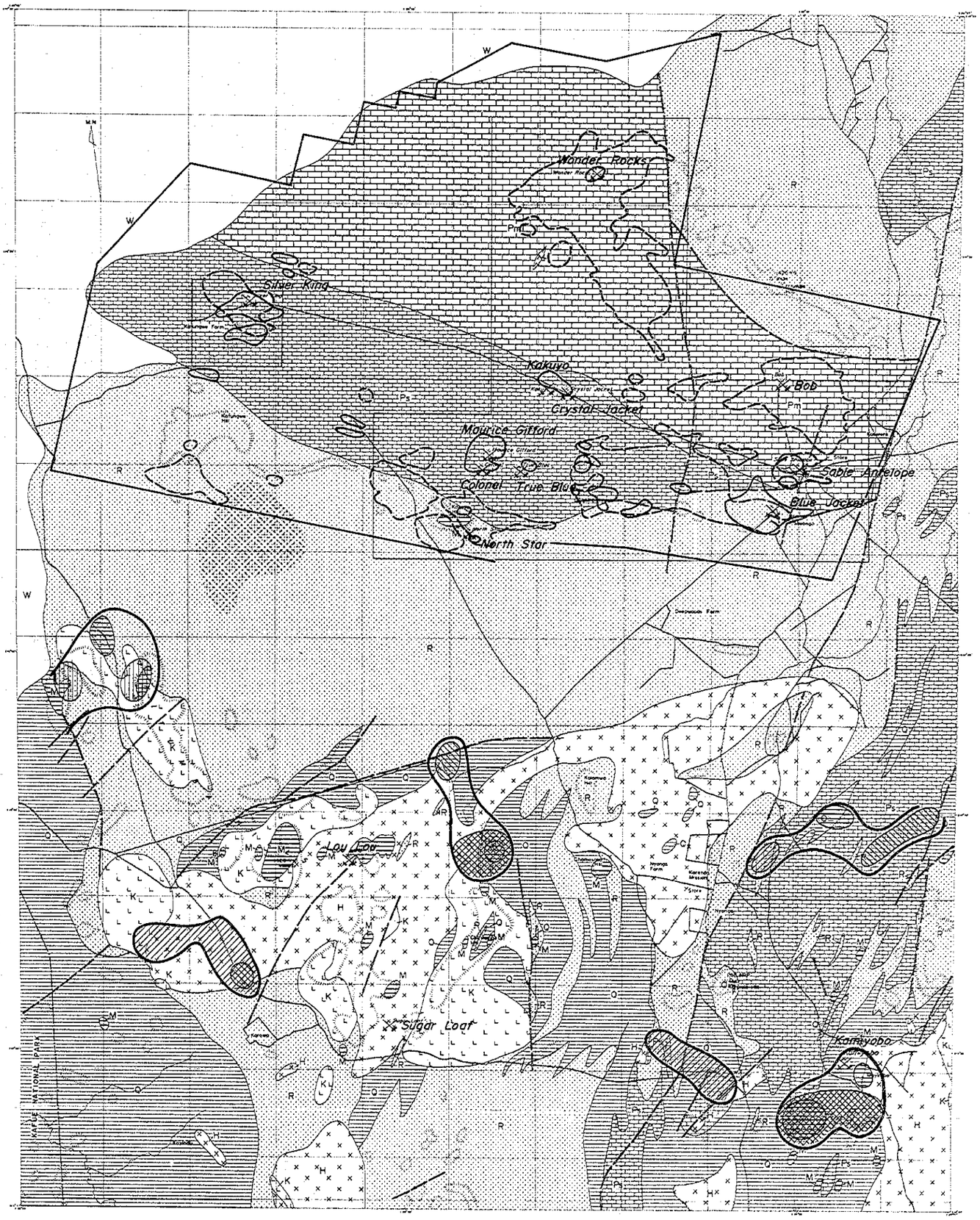

LEGEND

- Geochemical Anomalous Zone
- Cu : Over Critical Value (Threshold Value)
- Pb : 〃 (〃)
- Zn : 〃 (〃)
- Ag : 〃 (〃)
- Reanalysis of Old Data — Cu : Over Critical Value (Threshold Value)
- Reanalysis of Old Data — Zn : 〃 (〃)
- Disused Mine Site Or Mineralized Area
- Geochemical Surveyed Area By Mindeco Noranda Ltd.

(See Fig. Ⅱ-1 on Geological Legend)

Fig. Ⅲ-11 Distribution Map of Mineralized Areas

PART IV GEOPHYSICAL SURVEY (CSAMT)

PART IV GEOPHYSICAL SURVEY (CSAMT)

Chapter 1 General Description

The CSAMT (Controlled Source Audiofrequency Magnetotellurics) is a kind of magnetotelluric method using an artificial source of audiofrequency electro-magnetic energy and is recently being applied for resistivity mapping of massive sulfide and for geothermal exploration.

Frequent applications of the method rely upon its high ratio of signal to noise, rapid coverage of measurements and light weight of equipments. The source can be considered to be a plane wave if a transmitting station is located 3 to 5 skin depths apart from observation site, and thus field procedures and data processing techniques for interpretation are similar to those which are used in a conventional magnetotelluric method.

1-1 Objectives of the Survey

There are many abandoned mines such as the Sable Antelope, etc. in the area. But available data do not provide full information of geology, geological structure and mineralization.

Highly resistive limestones are widespread in the area and the CSAMT is applied to delineate anomalous zones of low resistivity, to clarify their properties and to investigate a spread and continuity of mineralization to the depths.

1-2 Location

The areas of present investigation are located about 200 km west-northwest of Lusaka and comprise two areas designated by A and B.

The area A covers some 75 km^2 where the Sable Antelope is situated and B covers an area of 4 km^2 in the vicinity of the Silver King. These mines are not being mined at present.

1-3 Specifications of the Survey

Specifications of the survey are as follows.

	A	B	Total
Observation stations	301	16	317
Transmitter sites	4	1	5
Frequency used	2048, 1024, 512, 256, 128 64, 32, 16, 8, 4 Hz		

The five combinations of transmitter sites with observation stations are shown in Table IV-1. The distances between a transmitter and observation stations are set more than 4 km apart in order to avoid an effect of 'near-field' curvature in the electromagnetic wave. Actual distance between a source and each station is given in the table of observation data.

Table Ⅳ-1 Transmitter and Observation Stations

Area	Transmitter	Dipole Length	Observation Stations	Total
A	No 1	1,500m	Nos 71~74, 81~91, 99~108, 117~127, 136~156, 164~185, 196~208, 213~220, 234~247, 266~270, 12, 252, 317	121
	No 2	1,500m	Nos 157~163, 186~195, 209~212, 221~233, 248~251, 253~265, 271~276, 277~289, 290~300	81
	No 3	1,500m	Nos 45~70, 75~80, 92~98, 109~116, 128~135	55
	No 4	1,500m	Nos 1~44	44
B	No 5	1,500m	Nos 301~316	16
			Total	Stations 317

1-4 Field Procedures

The observation stations were distributed densely in anomalous areas and sporadically in surrounding areas to cover the areas of anomalies which were obtained from the reprocessing of geochemical data, the distribution of these points and transmitter sites is illustrated in Fig. IV-1.

The datum point was placed at the Miumbe Hill of 1343 m a.s.l. The baseline was laid down after surveying the main road by using a pocket compass and tape. From the baseline, all stations were set in a manner of grid pattern.

At an observation site, a dipole spacing at 50 m is laid in parrelel with the transmitting dipole and an antenna is placed horizontally and at a right angle with the direction of dipole.

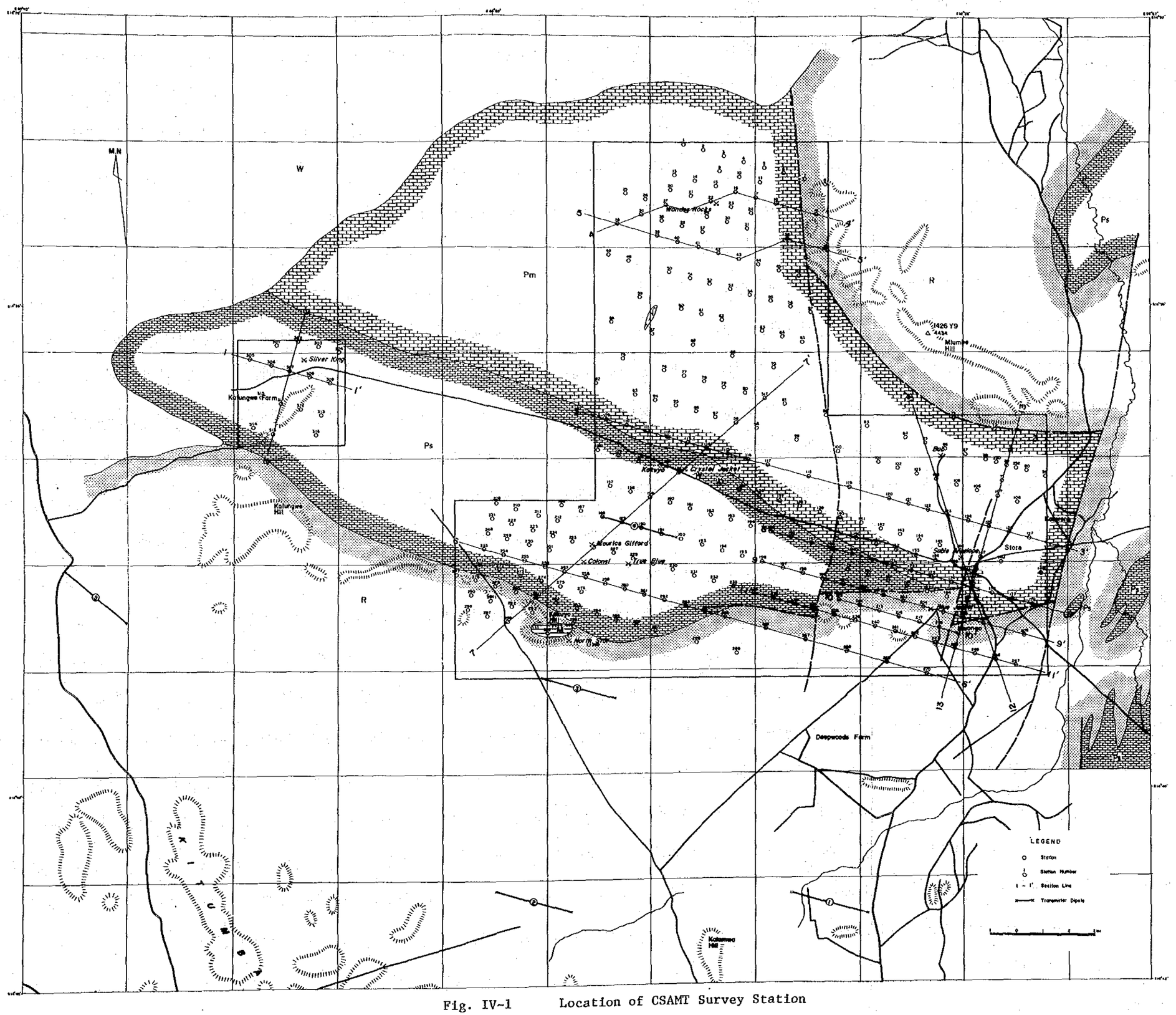

Fig. IV-1 Location of CSAMT Survey Station

The field Layout of the CSAMT survey is illustrated in Fig. IV-2. The measured parameters consist of the horizontal electric field Ex in a direction parallel to the transmitting source and the horizontal magnetic field Hy in a direction perpendicular to the source.

An apparent resistivity is calculated by

$$\rho_a = \frac{1}{5f}\left(\frac{Ex}{Hy}\right)^2 \quad \text{(ohm-m)} \quad \text{.....(1)}$$

where ρ_a : Apparent resistivity of the ground

f : frequency (Hz)

Ex : Horizontal electric field (mV/km)

Hy : Horizontal magnetic field (gamma)

The apparent resistivity obtained from the equation (1) is considered to show an average resistivity of the effective penetration depth $\delta/\sqrt{2}$ (δ: Skin depth). The skin depth means the depth at which the amplitudes of electric and magnetic fields have been attenuated to 1/e (or 37 percent) of the surface value, and is expressed in the equation (2).

$$\delta = 503\sqrt{\frac{\rho}{f}} \quad \text{(m)} \quad \text{..... (2)}$$

where ρ : Resistivity of the ground (ohm-m)

f : Frequency (Hz)

An effective penetration depth $\delta/\sqrt{2}$ varies depending on the resistivity of the ground and the frequency of electromagnetic wave.

An effective penetration depth for typical ground resistivities is given in Table IV-2.

For example, if an apparent resistivity of 1000 ohm-m is obtained with a frequency of 2048 Hz, the value indicates

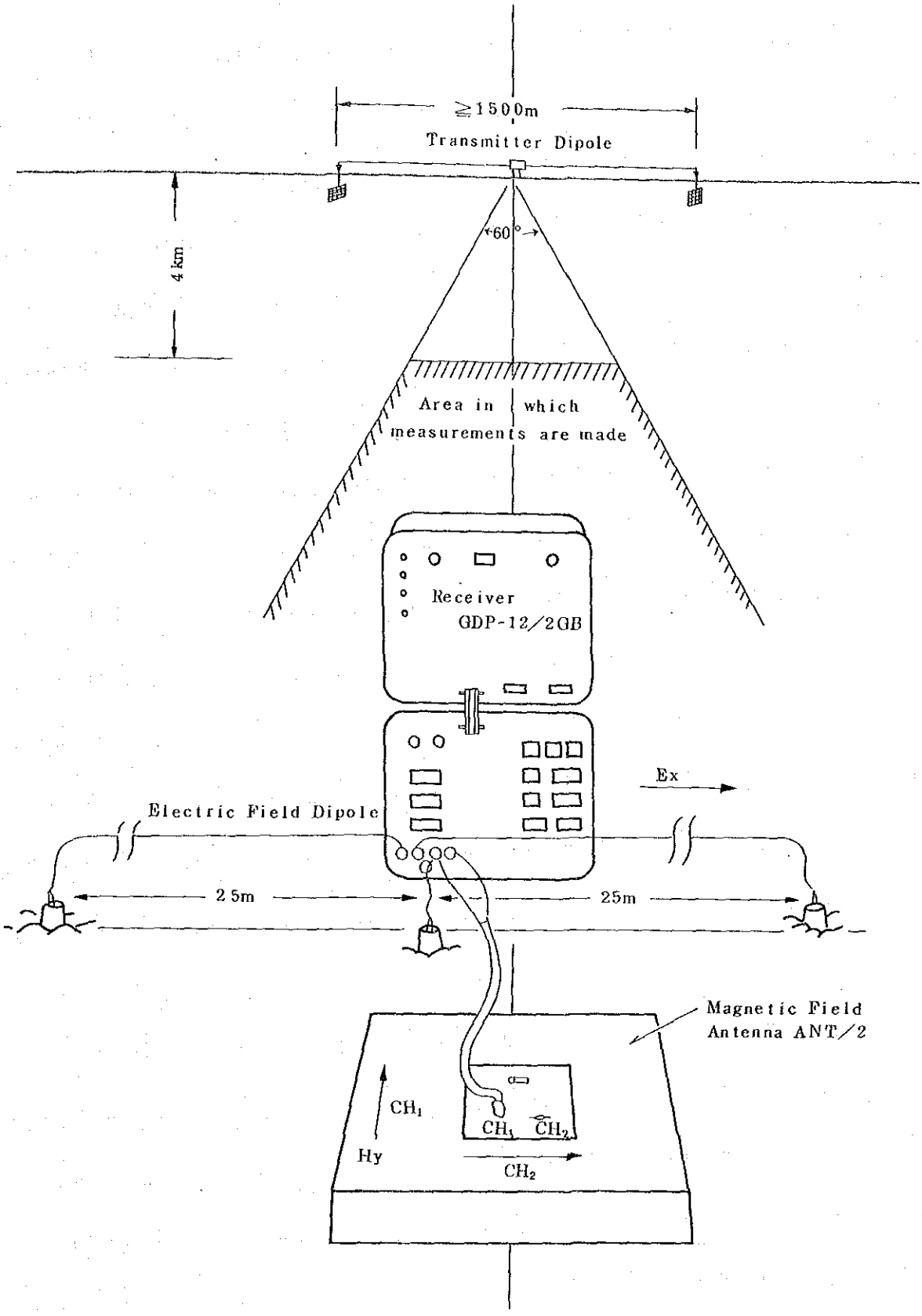

Fig. Ⅳ-2 Field Layout of a CSAMT Survey

the average resistivity to the depth of some 250 m.

Table Ⅳ-2 Effective Penetration Depth ($\delta/\sqrt{2}$: m)

	Resistivity (ohm-m)				
Frequency (Hz)	1	10	100	1,000	10,000
2,048	8	25	79	249	786
1,024	11	35	111	352	1,112
512	16	50	157	497	1,573
256	22	70	222	703	2,224
128	31	99	315	995	3,146
64	44	141	445	1,407	4,449
32	63	199	629	1,989	6,291
16	89	281	890	2,813	8,897
8	126	398	1,258	3,979	12,582
4	178	563	1,779	5,627	17,794

1-5 Equipments

The equipments are listed in Table IV-3 and a block diagram is shown in Fig. IV-3. In the field a current of square wave controlled by a frequency controller, is transmitted into the ground.

Measurements are made at the observation sites for amplitudes and phases of electric and magnetic fields. After being amplified, signals are digitized and stacked to improve the ratio of signal to noise. The apparent resistivity is calculated by a microcomputer in the receiver in accordance with the equation (1).

The apparent resistivity and the phase difference between Ex and Hy are displayed in the receiver and the outputs of data are printed by the cassette-printer.

Table IV-3 CSAMT Equipments

Equipment	Manufacturer	Model	Specification	Qty
Power Supply	Zonge (USA)	ZMG-20	Maximum Power : 20 kVA Alternator : 400 Hz 115V 3 Phase Engine : WISCONSIN 465D 62 HP	1
Regulator	Zonge	VR-1	Voltage Regulation	1
Transmitter	Zonge	GGT-20	Output voltage:400,600, 800,1,000V Output Current:Max 40A Square Wave Frequency : DC ~ 10 kHz	
Controller	Zonge	XMT-12	Frequency : DC ~ 2,048Hz	1
Receiver	Zonge	GDP-12/2GB	2 Channel Data Processor	1
Antenna	Zonge	ANT/2	Dual Axis Magnetic Field Detector	1
Cassette/Printer	Zonge	CAP-12	Printer : Minicassette	1

Chapter 2

Data Processing and Measurements of Physical Properties

2-1 Data Processing

The results are presented on the apparent resistivity map, the apparent resistivity and resistivity section, and the resistivity map.

The apparent resistivities at each frequency are plotted on a series of maps (Fig. IV-4 ~ IV-13). The apparent

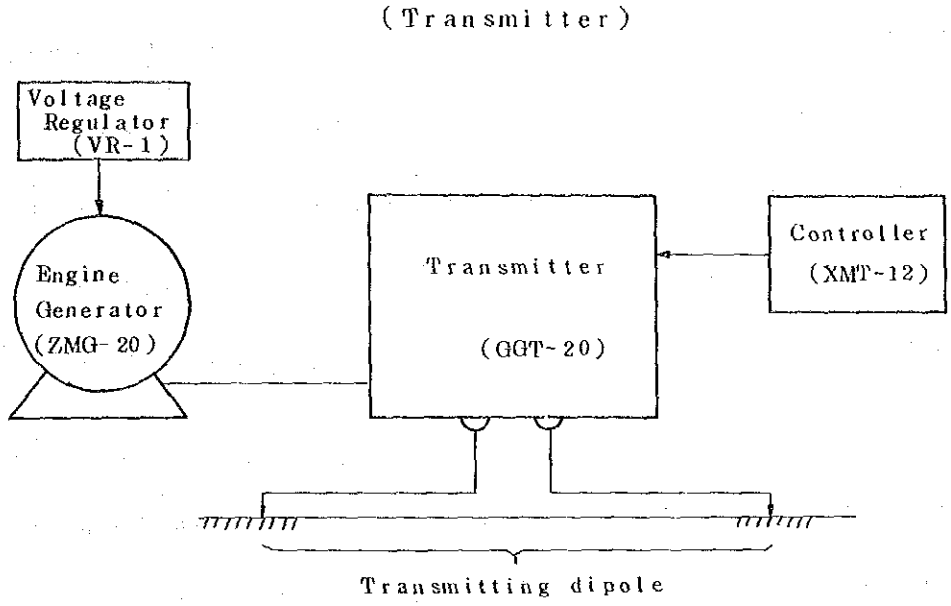

Fig. Ⅳ－3 Block Diagram of Zonge Survey System

Table IV-4 Resistivity and F.E. of Rock Samples

Sample No.	Rock, Ore	Resistivity (ohm-m)	Frequency Effect (%)	Location	Remarks
F 87	Bedded Limestone	8,492	< 1	Colonel	
F 144	Brecciated Massive Limestone	2,432	< 1	Sable Antelope	
F 152	Massive Limestone	9,384	< 1	Bob Zinc	
F 203	Brecciated Massive Limestone	3,723	< 1	Wonder Rocks	
F 84	Massive Limestone	6,880	< 1	Silver King	
T 18	Metasandstone	961	2.3		
T 14	Metasandstone	1,116	2.5		
T 93	Metasandstone	1,028	1.3	North Star	
T 61	Shale	1,273	1.3		
T 72	Quartz Porphyry	989	< 1		
T 53	Syenite	2,910	< 1		
T 62	Syenite	1,800	< 1		
F 141	Ore	15	42	Sable Antelope	Bornite,Chalcocite(Cu 26%)
F 14011	Ore	34	137	Sable Antelope	Bornite,Chalcocite(Cu 23%)
F 223	Ore	8,484	5.8	Crystal Jacket	Malachite (Cu 8%)
F 55	Ore	7,205	< 1	Kamiyobo	Limonite

resistivity section illustrates the apparent resistivities plotted on the diagram, of which the abscissa is locations of the stations, and the ordinate is frequencies.

The sounding data are analysed on the assumption of horizontally stratified multiple layers. The nonlinear least squares method is used and the results are complied on the CSAMT Sounding curves. The resistivity section is provided to show the analysed resistivities on the diagram, of which the abscissa is locations of the stations and the ordinate is depths (Fig. IV-14 to Fig. IV-18).

The resistivity map shows a distribution of resistivities at the same depth. Five maps of 0 m, -100 m, -200 m, -300 m, and -400 m are provided (Fig. IV-19 to Fig. IV-23). Intervals of contour lines are decided logarithmically on the basis of three intervals of long ρ_a per decade, being of 10, 21, 46, 100, 210, 460, 1000 and so on, because of the wide range of resistivity.

2-2 Physical Properties of Rock Samples

The resistivity and frequency effect of samples are given in Table IV-4. Samples are soaked in tap water for 72 hours and are provided for measurements.

Resistivity of rocks is high in limestones and low in syenites and metasandstones in descending order. The resistivity of ores which include sulphide minerals is low in general, but ores which comprise oxide minerals such as malachite have a high resistivity.

The frequency effect of rocks is very low except metasandstones. Also, the frequency effect of ores which consist mainly of limonite is low.

Chapter 3

Description and Interpretation of the Results

3-1 Apparent Resistivity Maps

The apparent resistivity maps are provided at the frequencies of 2,048, 1,024, 512, 256, 128, 64, 32, 16, 8 and 4 Hz.

(1) The map of 2,048 Hz (Fig. IV-4) shows characteristically a large contrast of the apparent resistivities ranging broadly from 10 to 20,000 ohm-m.

The values over the 1,000 ohm-m are dominant throughout the area A. A zone of low resistivity below the 100 ohm-m is located in the vicinity of the southeastern corner of the field. In general, the resistivity is high in limestones and low in the area of metasandstones and shales.

The contour line of 1,000 ohm-m roughly coincides with a lithological boundary of limestones with metasandstones and shales. The marks of L and H designate a local low or high respectively. A zone of high apparent resistivity over the 10,000 ohm-m was delineated in the central portion of the area A, trending WNW to ESE. A similar zone of over 10,000 ohm-m is located to the northwest of the area A, being probably correlative with massive limestones. Several zones of low resistivity below the 1,000 ohm-m in the area of limestones are noted as follows.

a. A zone at the northeast of Sable Antelope. A trend of NNE to SSW is conspicuous.

b. Four of small zones surrounding the Crystal Jacket.

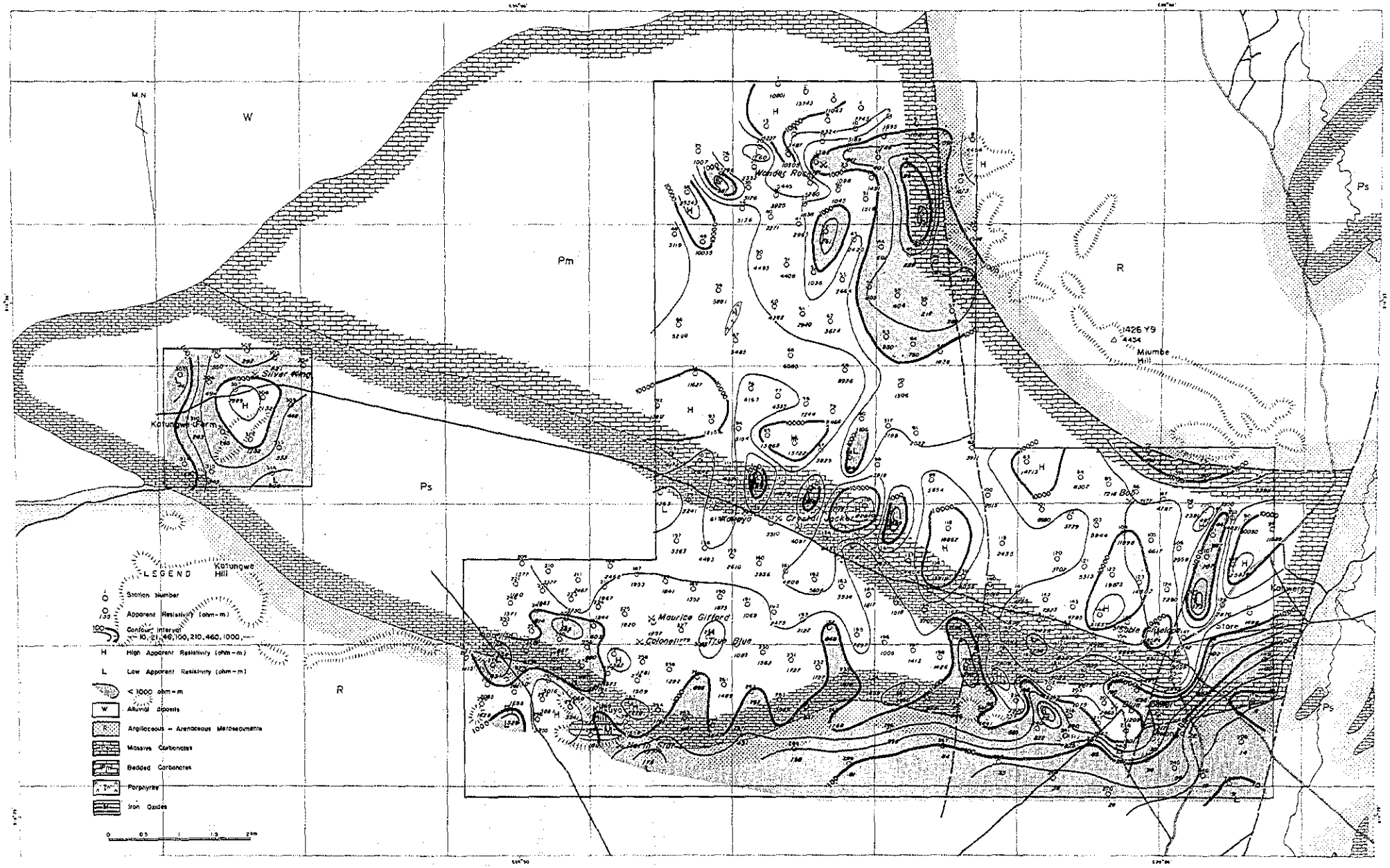

Fig. IV-4 Apparent Resistivity Map 2048 Hz

c. The zones at the east and west of Wonder Rocks. An east-west trending zone is devided at the center by a zone of high resistivity.

d. The zones at the south and southeast of Wonder Rocks. The zone at the southeast has a trend of north-south, and a fault trending north-south is delineated to the east of the zone.

e. A broad zone which trends east-westerly at the west of Colonel.

The areas at the south to the east of A provide a dominance of metasandstones and shales, and give low values of apparent resistivity.

The complicated patterns of contours at the south and the southeast spread over an area on the border of limestones with metasandstones and shales. An existence of faults or crushed zones can be expected.

Detected in these areas are seven localities of the zone of less than 1,000 ohm-m.

a. A zone trending toward northwest-westerly at the north of Blue Jacket.

b. A zone trending toward northwest at 1 km west of Blue Jacket.

c. A zone trending north-northwesterly at 2 km west of Blue Jacket.

d. A zone trending north-northwesterly at 2 km south-southeast of Crystal Jacket.

e. A zone at the south of True Blue.

f. A zone at the northeast of Bob Zinc.

g. A broad zone of less than 100 ohm-m at the south to the southeast of the area A, where metasandstones and shales are distributed.

The area B is underlain by stratified limestones and a zone of less than 100 ohm-m was detected at the west of area in the direction of north-south.

(2) Patterns delineated on the maps of 1,024, 512, and 256 Hz (Fig. IV-5 to Fig. IV-7) are very similar to those noted on the map of 2,048 Hz.

On the maps of 128, 64 and 32 Hz (Fig. IV-8 to Fig. IV-10), the values of apparent resistivity have a tendency to increase toward the west of the area A and decrease toward the east. On the maps of 16, 8 and 4 Hz (Fig. IV-11 ~ Fig. IV-13) a north-south trending structure of resistivity is apparent in the central parts of the area A. On the map of 2,048 Hz, the apparent resistivity ranges from 200 to 20,000 ohm-m in the vicinity of mineralized zones (Table IV-5).

Table IV-5 Apparent Resistivity around Ore Deposits

Ore Deposit	Apparent Resistivity (ohm-m)
Bob Zinc	4,640 ~ 10,000
Sable Antelope	10,000 ~ 21,500
Wonder Rocks	464 ~ 1,000
Crystal Jacket	2,150 ~ 4,640
Kakuyo	2,150 ~ 4,640
Maurice Gifford	1,000 ~ 2,150
Colonel	1,000 ~ 2,150
True Blue	2,150 ~ 4,640
Silver King	1,000 ~ 2,150
Blue Jacket	1,000 ~ 2,150
North Star	215 ~ 464

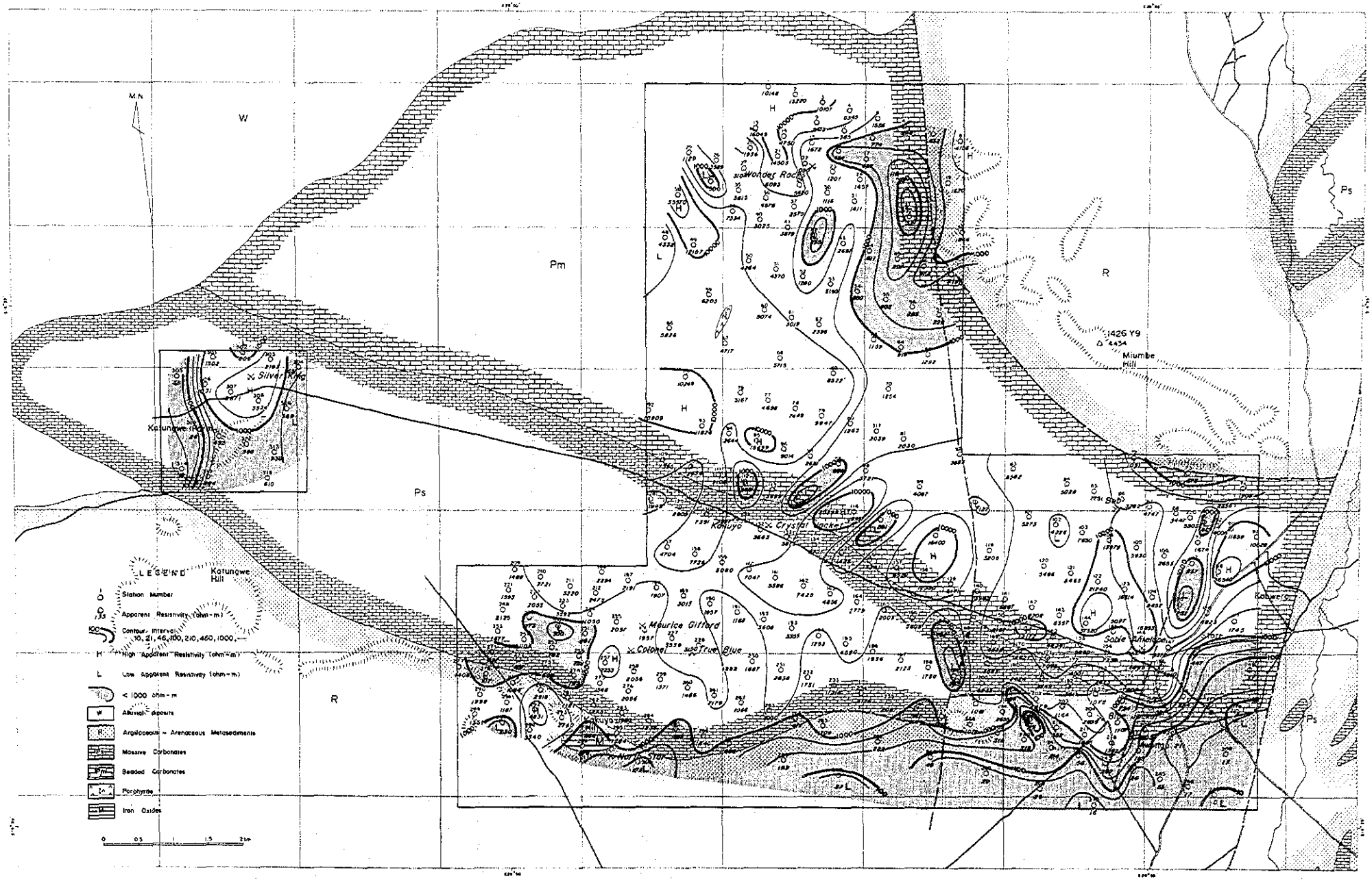

Fig. IV-5 Apparent Resistivity Map 1024 Hz

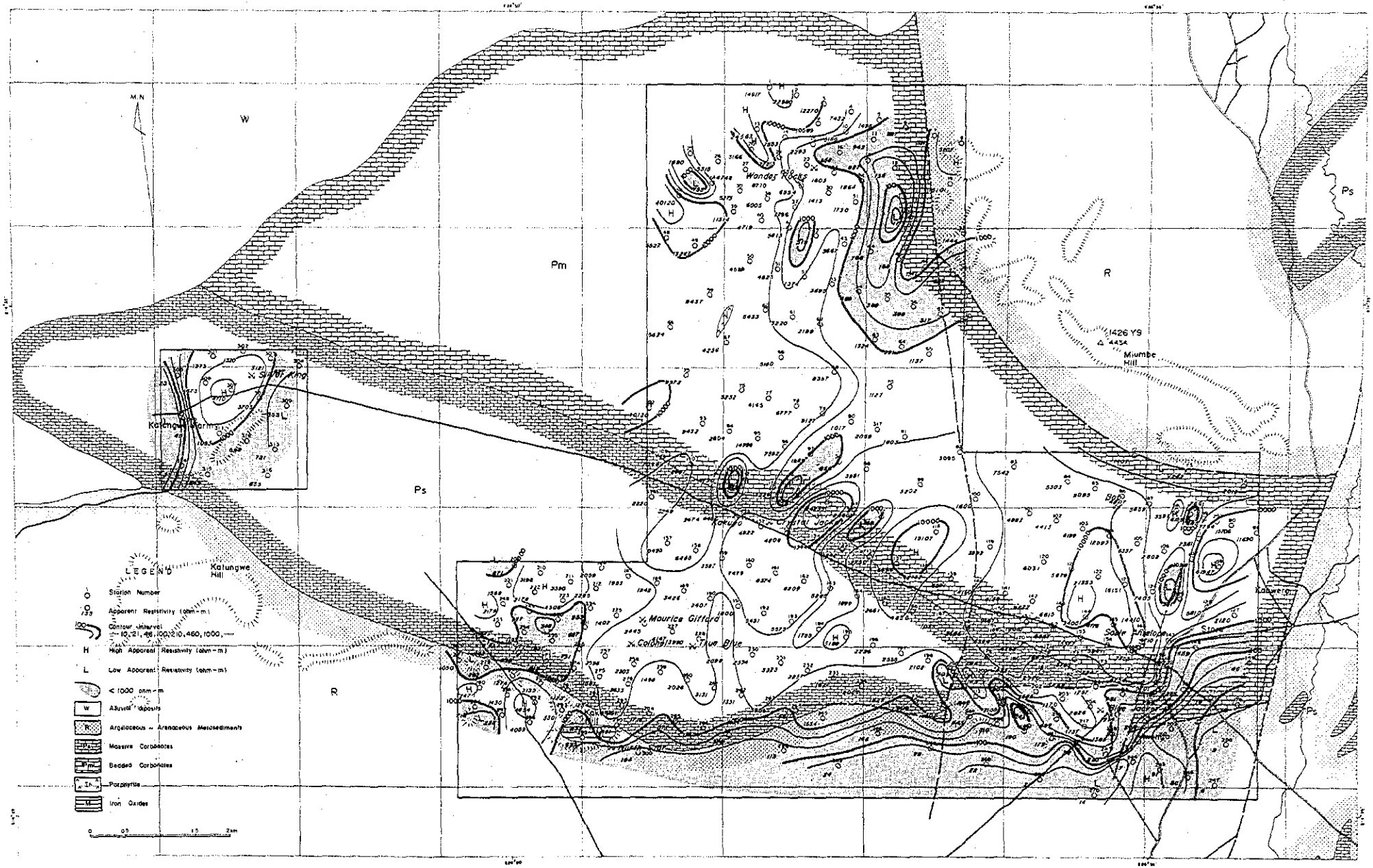

Fig. IV-6 Apparent Resistivity Map 512 Hz

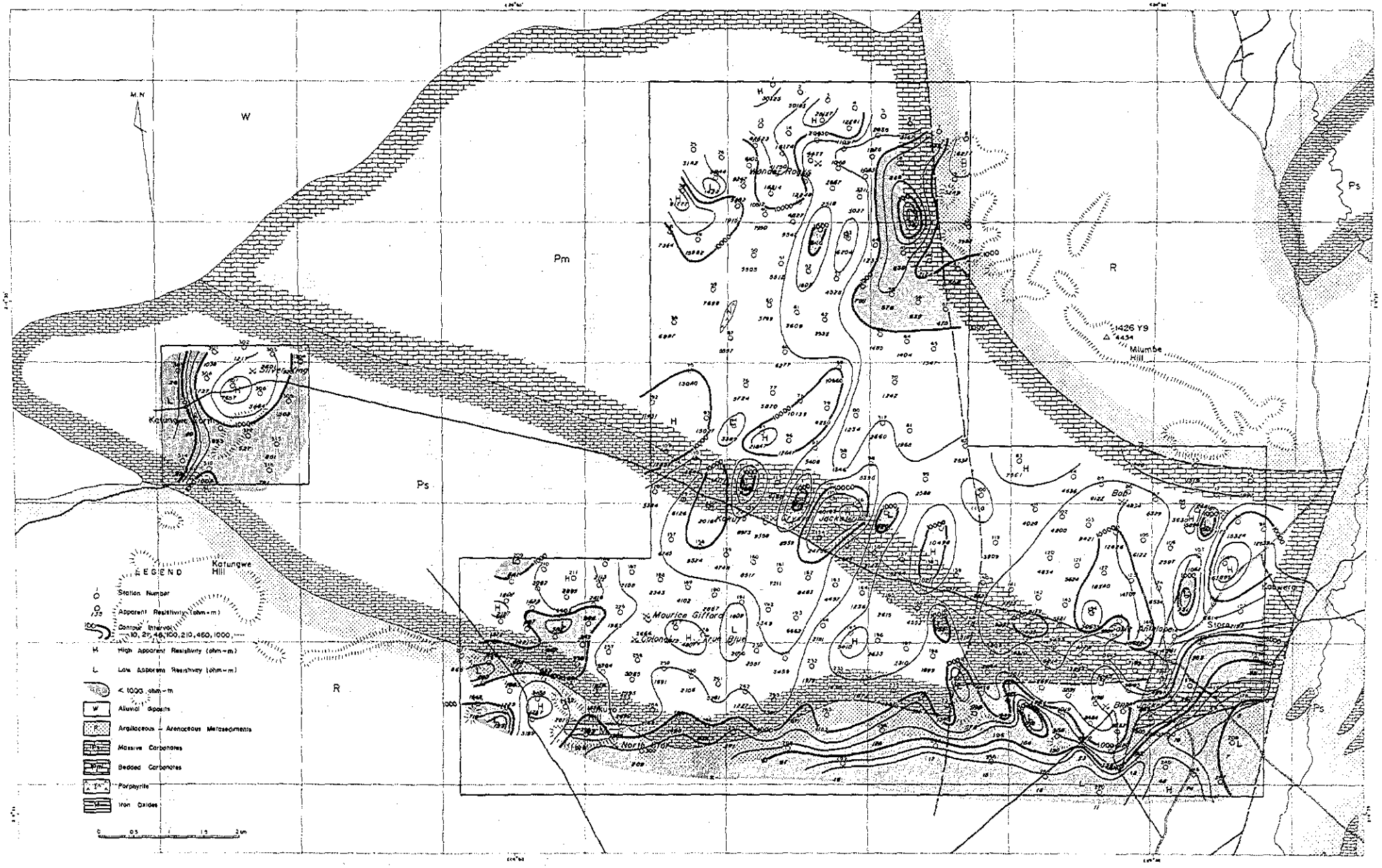

Fig. IV-7 Apparent Resistivity Map 256 Hz

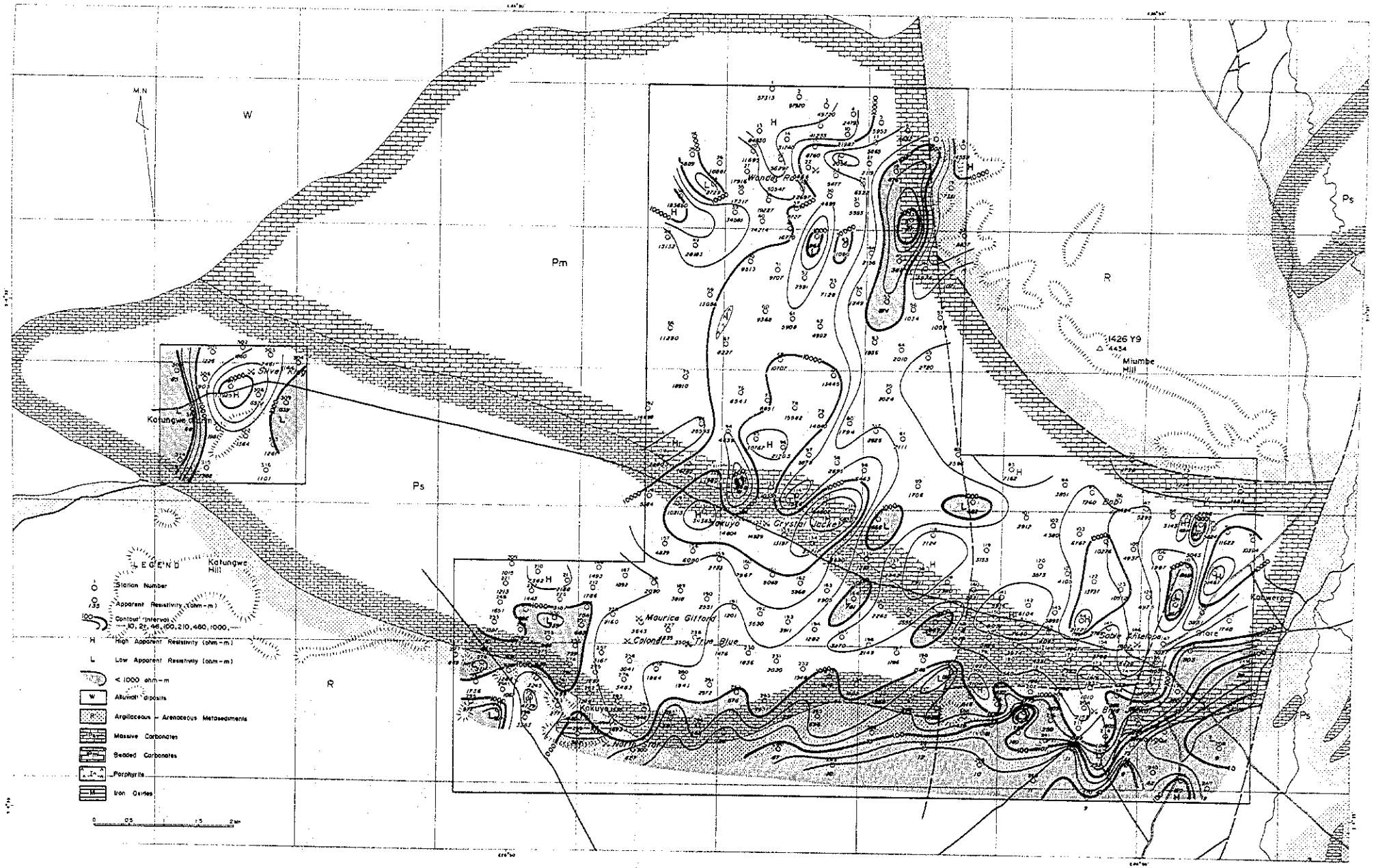

Fig. IV-8 Apparent Resistivity Map 128 Hz

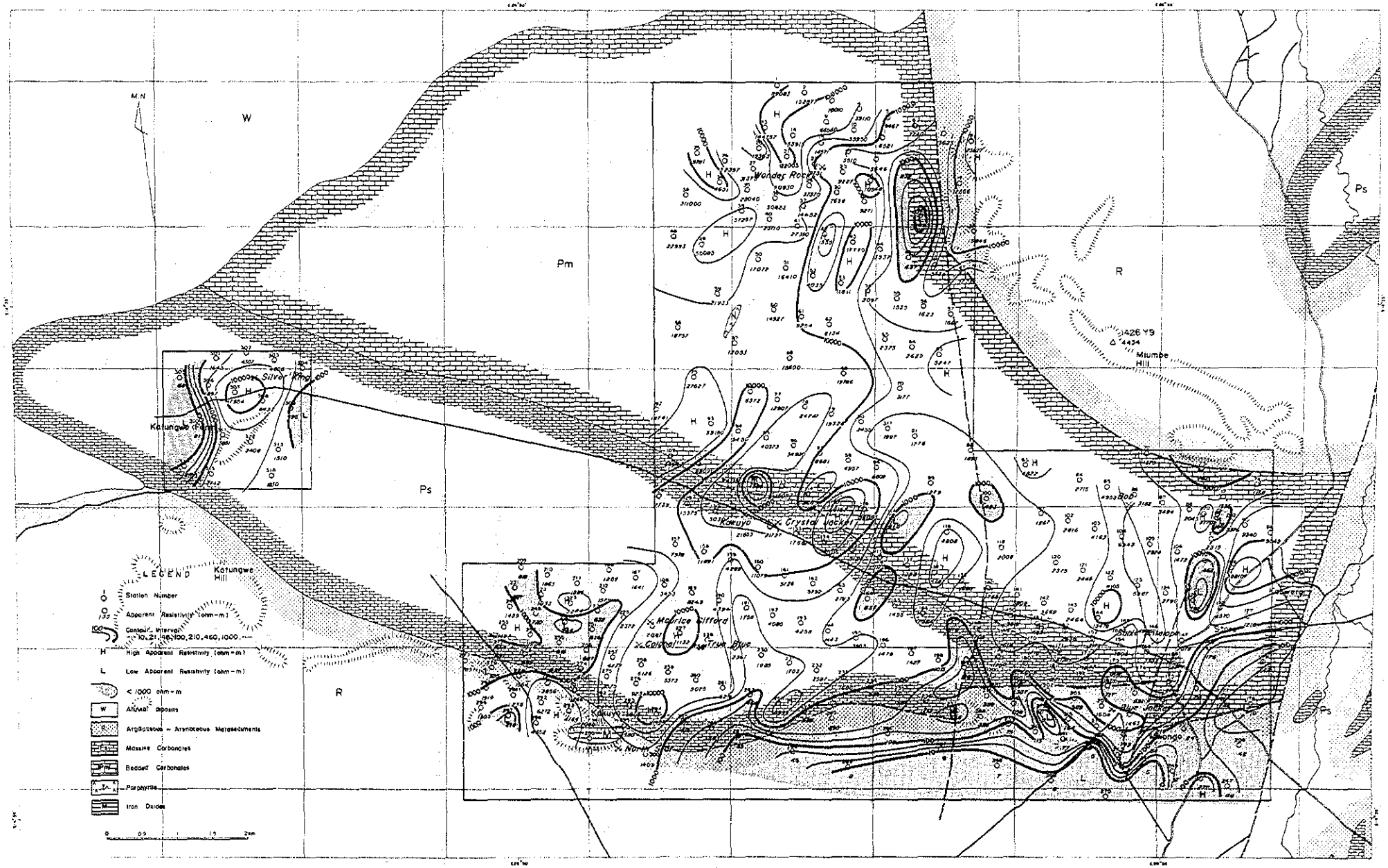

Fig. IV-9 Apparent Resistivity Map 64 Hz

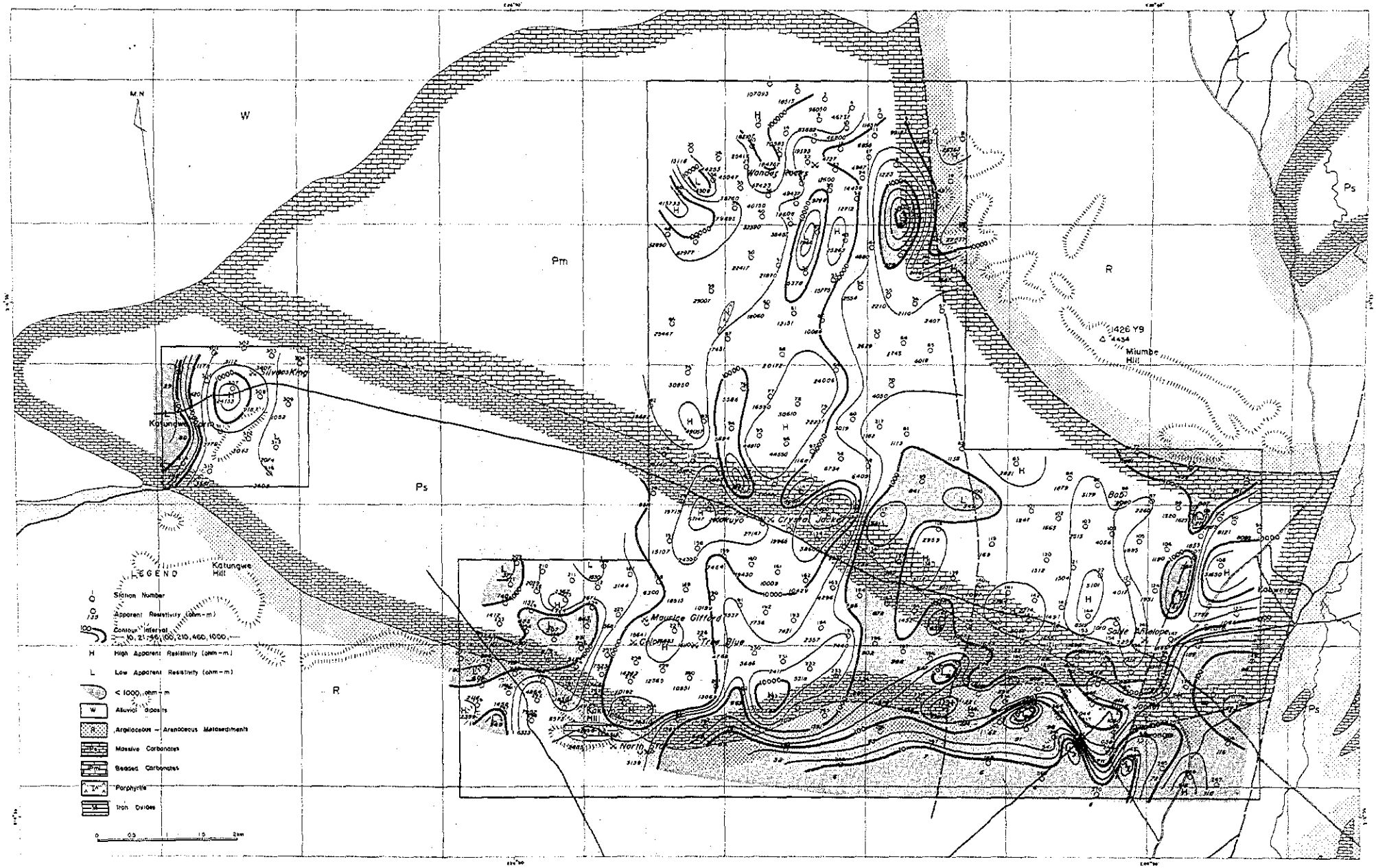

Fig. IV-10 Apparent Resistivity Map 32 Hz

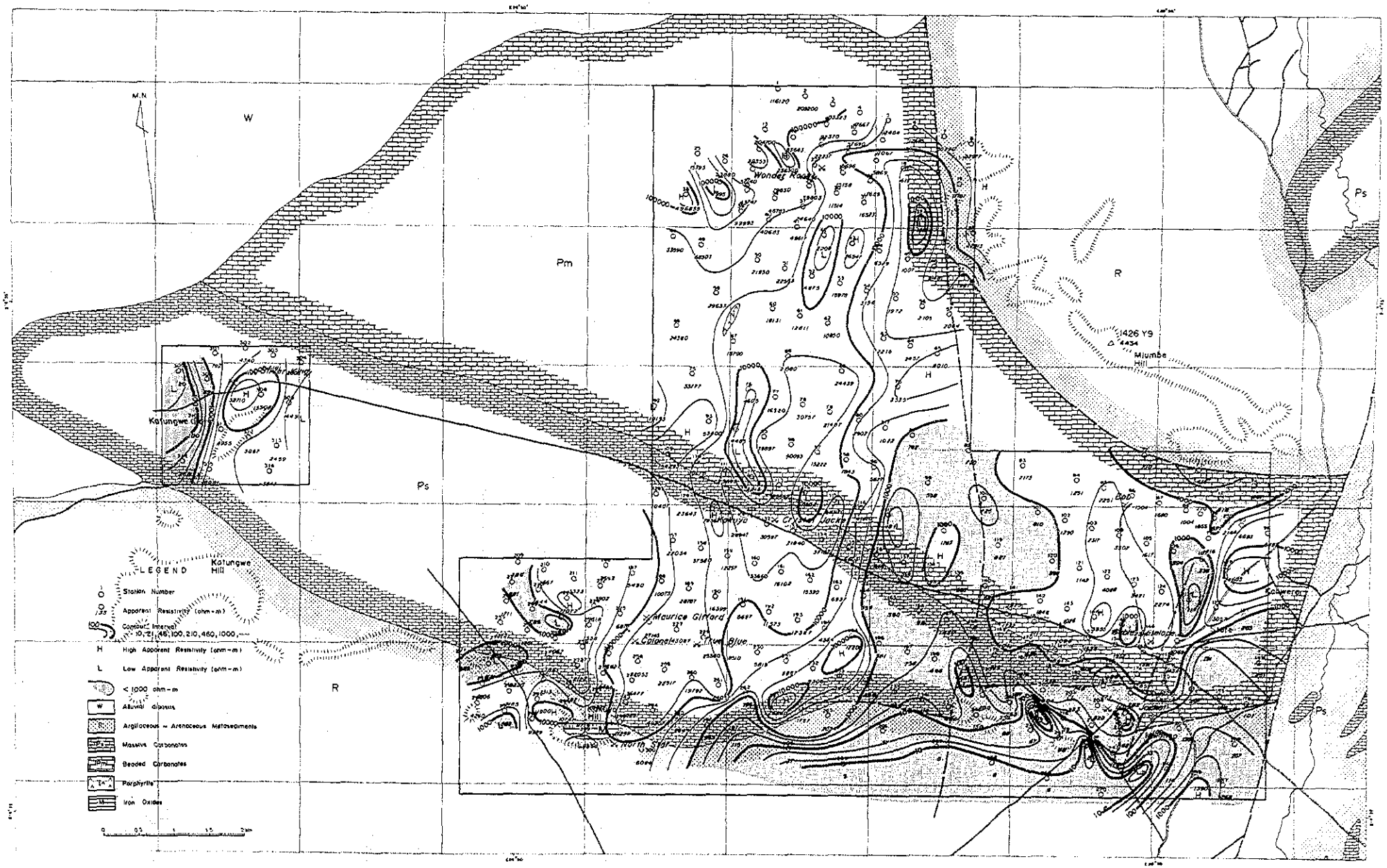

Fig. IV-11 Apparent Resistivity Map 16 Hz

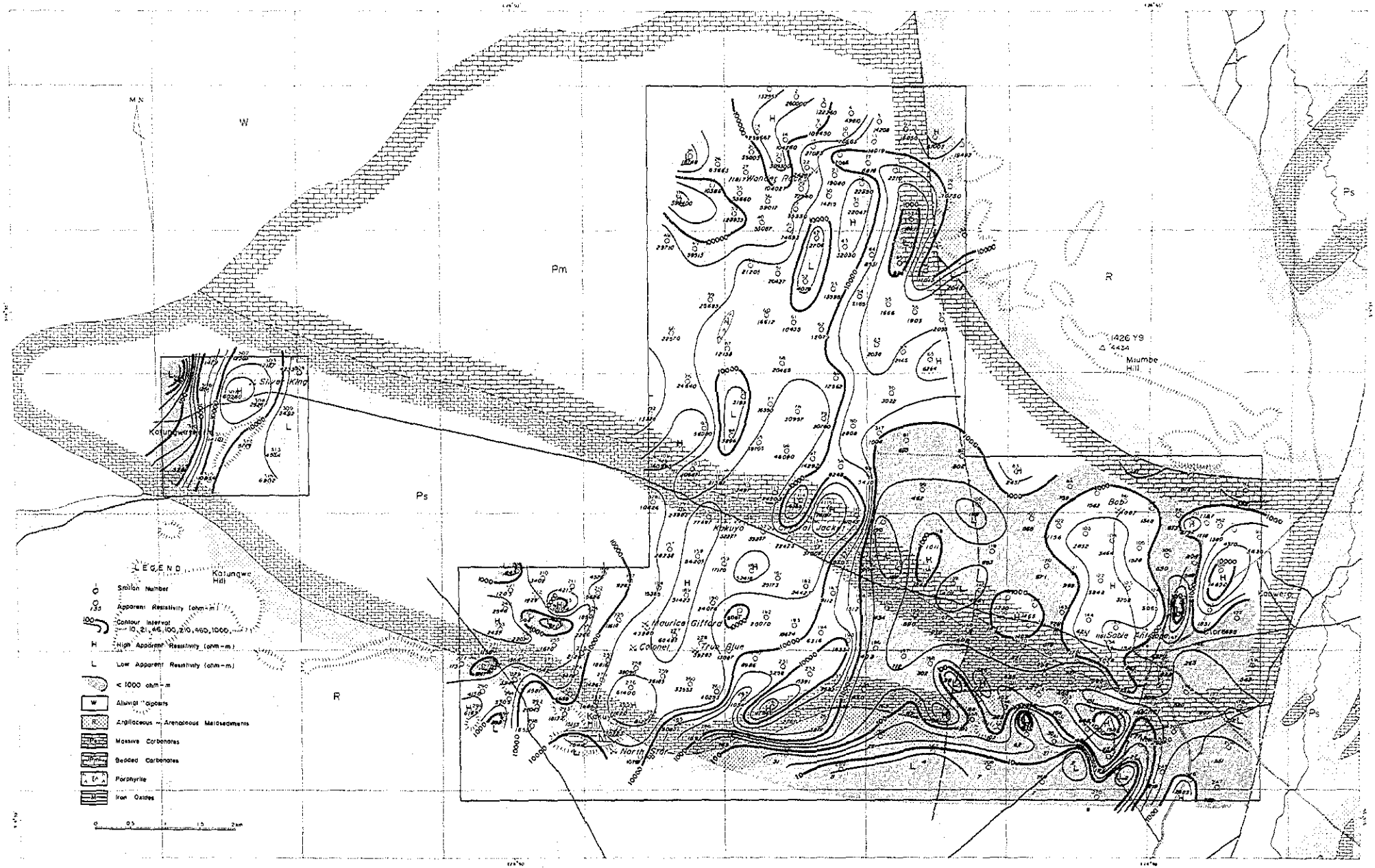

Fig. IV-12 Apparent Resistivity Map 8 Hz

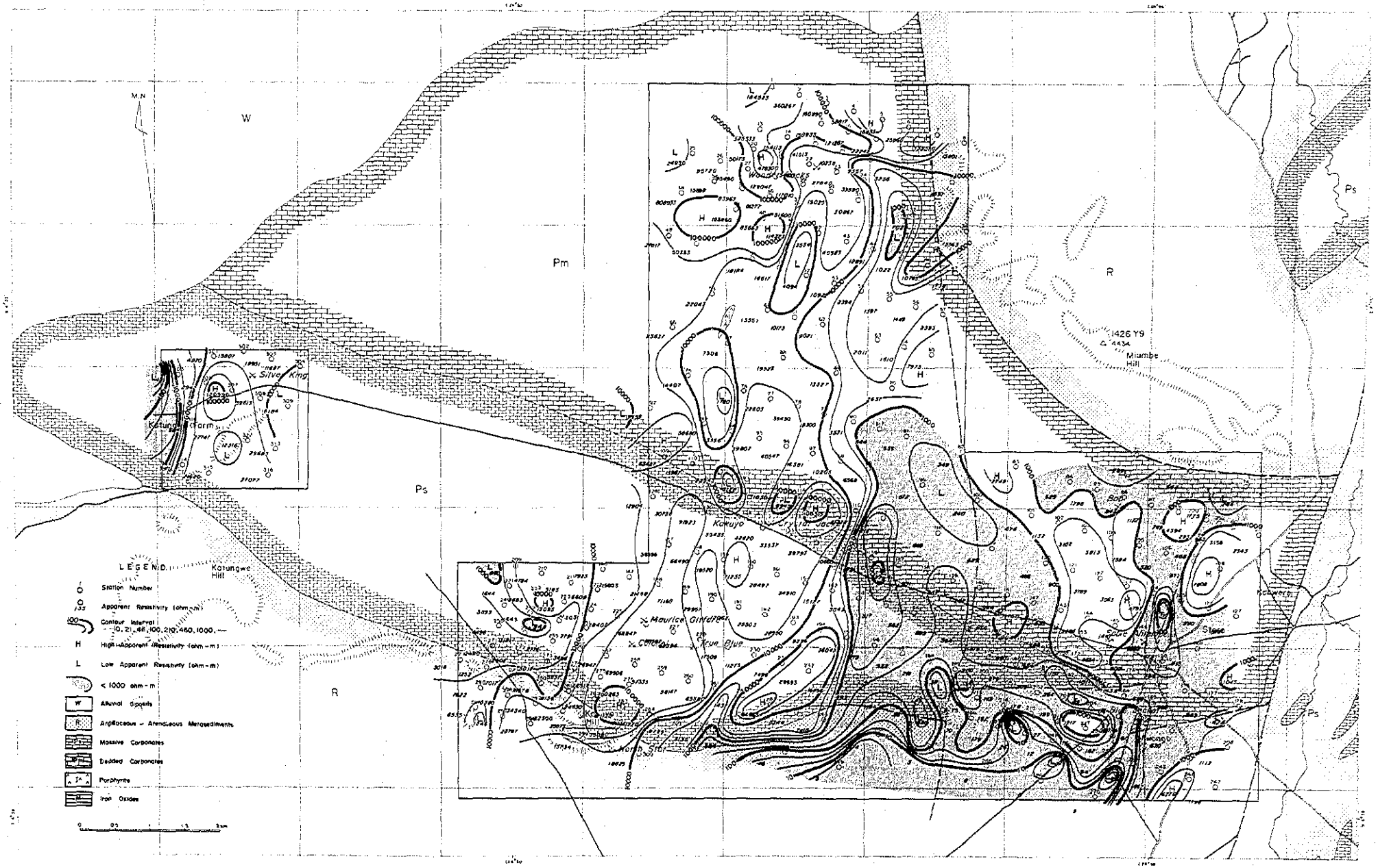

Fig. IV-13 Apparent Resistivity Map 4 Hz